THE EFFECT OF VIBRATORY SCREENS ON SUPPORTING STRUCTURES

by

Esra Hasanbas

A thesis submitted to the faculty of
The University of Utah
in partial fulfillment of the requirements for the degree of

Master of Science

Department of Civil and Environmental Engineering

The University of Utah

May 2013

The University of Utah Graduate School

STATEMENT OF THESIS APPROVAL

The thesis of **Esra Hasanbas**

has been approved by the following supervisory committee members:

Luis Ibarra	, Chair	**12/5/2012** Date Approved
Chris Pantelides	, Member	**12/5/2012** Date Approved
Paul McMullin	, Member	**12/5/2012** Date Approved

and by **Chris Pantelides** , Chair of

the Department of **Civil and Environmental Engineering**

and by Donna M. White, Interim Dean of The Graduate School.

ABSTRACT

The consideration of the dynamic effects of vibrating mineral separators on its supporting structure is crucial to design a reliable structural support system. This study evaluates the dynamic response of steel frame structures subjected to harmonic vibrations caused by mineral separators (screens). The goals of this study are to determine the parameters controlling the structural response of the supporting system, and to provide practical methods to reduce the vibrations on the steel frames at the design stage.

In this study, the behavior of a steel frame structure supporting a vibrating screen was investigated through numerical analyses and field experiments. The dynamic response of the supporting frame structure recorded from field experiments was compared to computer-based dynamic analysis results. For this purpose, structural models were developed in the software program SAP2000 to predict the dynamic behavior of the supporting steel frames under harmonic vibrations; whereas, during the field experiments, accelerometers recorded the steel frames' vertical and horizontal dynamic response.

The results indicate that the harmonic vibrations caused by the screen can cause large dynamic amplifications in the vertical direction for expected floor fundamental frequencies. Because the system's natural frequency depends on its mass and stiffness, excessive vibration in the supporting structure can be controlled by using passive vibration control methods such as isolators, dampeners and structural design modifications. In this thesis, modification of the structural dynamic properties was the only option investigated due to several restrictions on the other options. Thus, the selected design options depend

on the magnitude of the ratio of forcing frequency of the screen and the natural frequency of the system f/f_n.

For the systems investigated, vertical vibrations can be evaluated in isolation considering only the bay where the screen is located. The simply supported beams tend to isolate the vertical vibration from the rest of the structure. Whereas vertical vibrations are a local phenomenon, horizontal vibrations are usually affected by the overall building's response. Finally, it was concluded that the weight of the material in the screen has a negligible effect on the system's frequency, even in the vertical direction.

To Mom

TABLE OF CONTENTS

LIST OF FIGURES

LIST OF TABLES

ACKNOWLEDGEMENTS

I would like to express my sincere gratitude to Dr. Luis Ibarra for the perceptive instructions, support and motivation. I am so grateful to his guidance which helped me to achieve my educational goals. I would like to thank Dr. Paul McMullin for the constant help, guidance and insightful suggestions and I am grateful to Dr. Chris Pantelides for his influential assistance.

I am thankful to Structural Group of Millcreek Engineering for their support and help throughout my research.

I also would like to thank Necati Celik who trusted me and encouraged me to start this journey.

Finally, I would like to thank my family and my friends, Joel Parks and Sharad Dangol for their continued support and words of encouragement.

1. INTRODUCTION

1.1. Background

Harmonic loading caused by rotating machinery can lead to excessive vibration in steel frames, which might result in failure of the system. This study evaluates the behavior of steel frame structures subjected to dynamic loading caused by vibrating mineral separator, also known as screens.

The research focuses on industrial steel frame structures with no rigid diaphragms. The goal of this thesis is to provide practical methods to reduce vibrations on the steel frames. In early 20th century, several analytical methods were developed to address the problem of vibration behavior and control of machines. However, it was observed that reliable experimental data was necessary to develop accurate analytical methods (Arpaci, 1996).

The screen evaluated in this study is supported by a steel frame structure in a mine facility. The evaluated structure experienced excessive vibration after the construction was completed and the screen started operations. The industrial plant was shut down due to the excessive vibrations transferred from the screen to its supporting frame. Computer-aided dynamic analyses were used to determine the vertical and horizontal dynamic response of the system. Field experimental tests recorded the motion of the empty screen by using accelerometers with data loggers. The system's dynamic response was also recorded when the mineral separator (screen) was run with material. The effect of the material on the dynamic response was obtained by comparing the dynamic response for the empty screen and screen with material.

The dynamic response of steel frames that support screens depends on the static response and the amplification of this response due to dynamic loading. In this study, practical design solutions to prevent excessive vibration transferred from the screen to its supporting frame are researched. One practical method to reduce the vibrations on the steel frame is to use vibration isolators or dampeners which reduce the transmission of the harmonic force generated by the screen. This solution, however, is commonly used for the screens with comparatively higher operating frequencies. The screen used in this study has a horizontal operating frequency of 3.43 Hz and a vertical frequency of 6.87 Hz. Therefore, due to its low operating frequency, vibration isolation is challenging. For instance, ROTEX manufacturer conducted several experiments to analyze the dynamic response of the screen and its supporting frame when the transferred vibration is reduced by isolators, such as a spring and an isolator pad. The experiments were not successful because the screen could not accelerate through the natural frequency of the isolation system without exciting the isolators, which caused excessive vibration in springs and shearing of the rubber pads. The manufacturer trialed other experiments on isolators; however, none of them were successful. For that reason, the manufacturer does not recommend the use of isolators on Rotex screens.

Another practical design solution is modification of structural design, which is the alternative researched in this paper. The response of both a weak and a strong supporting frame is compared, as well as the effects of changing the system's mass and stiffness properties.

In addition, screen corrective actions should be carried out expeditiously because the mine facility has to be shut down if any of the screens stop running, resulting in large downtime losses. Thus, a reliable design criterion is essential for the dynamic performance of the steel frame structures that support vibratory screens.

1.2. Literature Review

Early research on vibration control focused on passive vibration control systems (Ormondroyd and Hartog, 1928), which can be based on dampers, shock absorbers, stiffeners, or modification of dynamic properties of the structural support system. Research on the behavior of the supporting structure of vibrating screens is scarce.

For instance, Allis Chalmers Mining Screen Company (1968) evaluated the effects of vibrating screens on their supporting structures, which were calculated by analyzing the members of the supporting system separately and then combining the data acquired from each member. However, considering each member separately and combining the natural frequency of each member in the supporting system can only provide limited answers. Although there are some limitations, this method is used by structural engineers vastly. Ronlov (1962) evaluated the vibration problems in processing plants, and he treated the whole support structure as a spring and the vibrating machinery as a single mass lumped to the spring. The structure was assumed to be a single-degree-of-freedom (SDOF) system; therefore, the dynamic response of multi-degree-of –freedom (MDOF) systems were limited to the response of SDOF systems. That is, the dynamic effect of higher-order modes was disregarded.

Dynamic analysis of elevated steel frame structures where the vibratory machinery was allocated were studied by Assunçăo (2009). He studied a framed structure supporting an unbalanced machine and concluded that a developed numerical model is suitable to evaluate the effects of vibrating mass on dynamic responses of the frame structure. However, the accuracy of the computational models by comparing them with the field results was disregarded. A practical solution to the excessive vibration caused by screens is a market need in the construction of industrial plants because few studies have investigated methods to modify the structural dynamics properties at the design stage.

2. BASIC PRINCIPLES OF HARMONIC MOTION

Harmonic loads are sinusoidal cyclic functions. The harmonic load caused by an unbalanced rotating machine is the most common example of periodic loads. Rotex Screen (Rotex 2012) generates periodic harmonic forces loads. Therefore, a proper sinusoidal time-history function should be input during the dynamic analysis.

2.1. Fundamentals

Undamped SDOF system response can be defined as: The equation of motion of an undamped SDOF system subjected to a dynamic force $P(t)$ can be expressed as:

$$m\ddot{u}(t) + ku(t) = P(t) \qquad (2.1)$$

where

$u(t)$: Displacement of SDOF system as a function of time (t)

$\ddot{u}(t)$: Acceleration of SDOF system as a function of time (t)

m : Mass of the system

k : Stiffness of the system

For harmonic loading, $P(t)$ is expressed as:

$$P(t) = P_o \sin(\omega t) \qquad (2.2)$$

where

P_o : Maximum static load on the structure

ω : Circular forcing frequency (rad/s)

If $P(t) = 0$, Equation (2.1) becomes a homogeneous differential equation that predicts the response for a free vibration regime. The response of the system can be

determined by applying the standards methods to solve a homogeneous differential equation. On the other hand, if a system is forced harmonically, the equation of motion becomes a non-homogeneous differential equation (Equation (2.1)). The solution to the non-homogeneous equation consists of a particular solution and a complementary solution. The particular solution corresponds to the steady-state solution; whereas the complementary solution is the response to the homogenous equation and stands for the transient solution. The transient part of the total response depends on the initial conditions of the system, such as initial displacement and velocity of the mass due to the sudden application of the external force. Transient response can be disregarded when the initial displacement and velocity are close to zero. In addition, the transient response is usually dissipated within the first few cycles after the force is applied. However, the steady-state response is always present in the system's total response. Figure 2.1 is an example of a total response of a system.

An undamped SDOF is the simplest structure that can be subjected to harmonic loading. Since the structure investigated is a steel frame building with no rigid diaphragms, the damping of the system is actually very low. Therefore, the solution for undamped SDOF system provides good insights on the vertical accelerations of the evaluated steel frames.

The solution for an undamped system under harmonic loading is as follows (Chopra, 2012):

$$u(t) = u(0)cos\omega_n t + \frac{\dot{u}(0)}{\omega_n} sin\omega_n t - \frac{P_o}{k}\frac{\omega/\omega_n}{1-(\omega/\omega_n)^2} sin\omega_n t + \frac{P_o}{k}\frac{1}{1-(\omega/\omega_n)^2} sin\omega t \qquad (2.3)$$

where

$u(0)$: Initial displacement

$\dot{u}(0)$: Initial velocity

ω_n : Circular natural frequency (rad/sec)

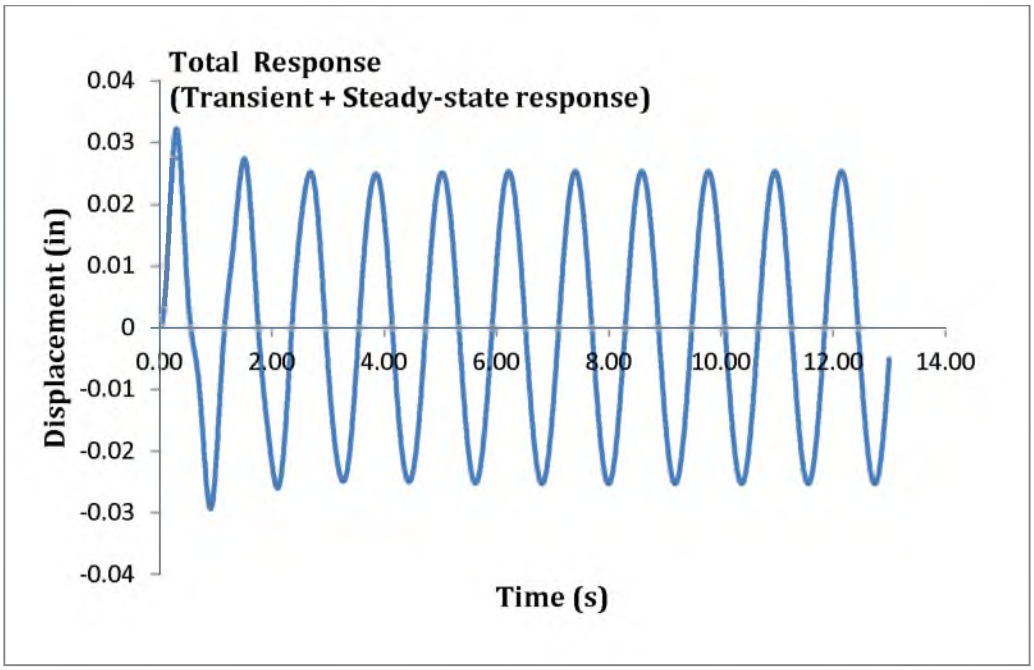

Figure 2.1 – Response of Damped System to A Harmonic Force

The static displacement $(u_{st})_o$, is expressed as:

$$(u_{st})_o = \frac{P_0}{k} \tag{2.4}$$

The first two terms of the solution of undamped SDOF systems (Equation 2.3) represent the transient response due to the initial system conditions, whereas the third term is the transient response due to the applied forces. The third term is a function of the static deformation (see Equation 2.4) and the ratio of the forcing frequency to natural frequency of the system. The transient part of the total response diminishes after a few cycles.

The last term of the total response equation (Equation 2.3) is the steady-state response of the system. The steady- state response is the only part of the solution that remains as long as the force is present. In most evaluations of rotating machinery, the steady- state response provides the only significant contributions to the total dynamic response, and Equation 2.3 can be reduced to:

$$u(t) = \frac{P_o}{k}\frac{1}{1-(\omega/\omega_n)^2} sin\omega t \quad (2.5)$$

Damped SDOF system response can be defined as: Steel frames for industrial plants usually exhibit low percentage of critical damping values ($\xi \approx 1\%$). The equation of motion for damped SDOF systems is shown in Equation (2.6).

$$m\ddot{u}(t) + c\dot{u}(t) + ku(t) = P(t) \quad (2.6)$$

The steady-state response for damped SDOF systems under harmonic loading is:

$$u(t) = (u_{st})_o R_d(sin\omega t - \varphi) \quad (2.7)$$

As observed, the response of a system to harmonic load is a function of its static deformation and an amplification factor, as described below.

2.2. Dynamic Amplification Factor (R_d)

The deformation response factor represents the dynamic amplification of the static displacement:

$$R_d = \frac{u_o}{(u_{st})_o} \quad (2.8)$$

u_o: Amplitude of dynamic deformation

The dynamic amplification factor, or deformation response factor (R_d), is a function of the ratio of the forcing frequency to the natural frequency of the system, and the system's damping. Equation (2.9) below represents the amplification factor in terms of the circular forcing frequency to circular system frequency ratio, and the damping ratio.

$$R_d = \frac{1}{\sqrt{\left[1-\left(\omega/\omega_n\right)^2\right]^2 + \left[2\xi\left(\omega/\omega_n\right)\right]^2}} \quad (2.9)$$

As R_d approaches to the unity, the expression for the amplification factor reduces to $R_d = 1/2\xi$, a value that is very close to the peak R_d for low-damped systems.

The forcing and system's natural frequencies can be expressed as:

$$f = \frac{\omega}{2\pi}$$

$$f_n = \frac{\omega_n}{2\pi}$$

where

f: Forcing frequency (Hz)

f_n : Natural frequency (Hz)

The amplification factor is re-written in terms of forcing frequency and natural frequency as follows:

$$R_d = \frac{1}{\sqrt{\left[1-\left(f/f_n\right)^2\right]^2+\left[2\xi\left(f/f_n\right)\right]^2}} \qquad (2.10)$$

$$f_n = \frac{1}{2\pi}\sqrt{\frac{k}{m}} \qquad (2.11)$$

As observed in Equation (2.11), the natural frequency of a system is a function of its stiffness (k) and mass (m). For instance, the system's natural frequency increases as k increases.

The system's frequency is very important to the dynamic response because as the forcing-to-system frequency ratio (f/f_n) approaches to the unity, the R_d parameter increases (i.e., resonance regime) and the dynamic displacement significantly increases. Figure 2.2 shows the f/f_n effect on the amplification factor for a system with a percentage of critical damping $\xi = 1\%$. As can be seen, for $\xi = 1\%$ the static response can be amplified 50 times (i.e., R_d =50, according to Equation 2.10) when f/f_n = 1.0. To prevent large R_d values that lead to resonance, the frequency ratio should not be close to the unity.

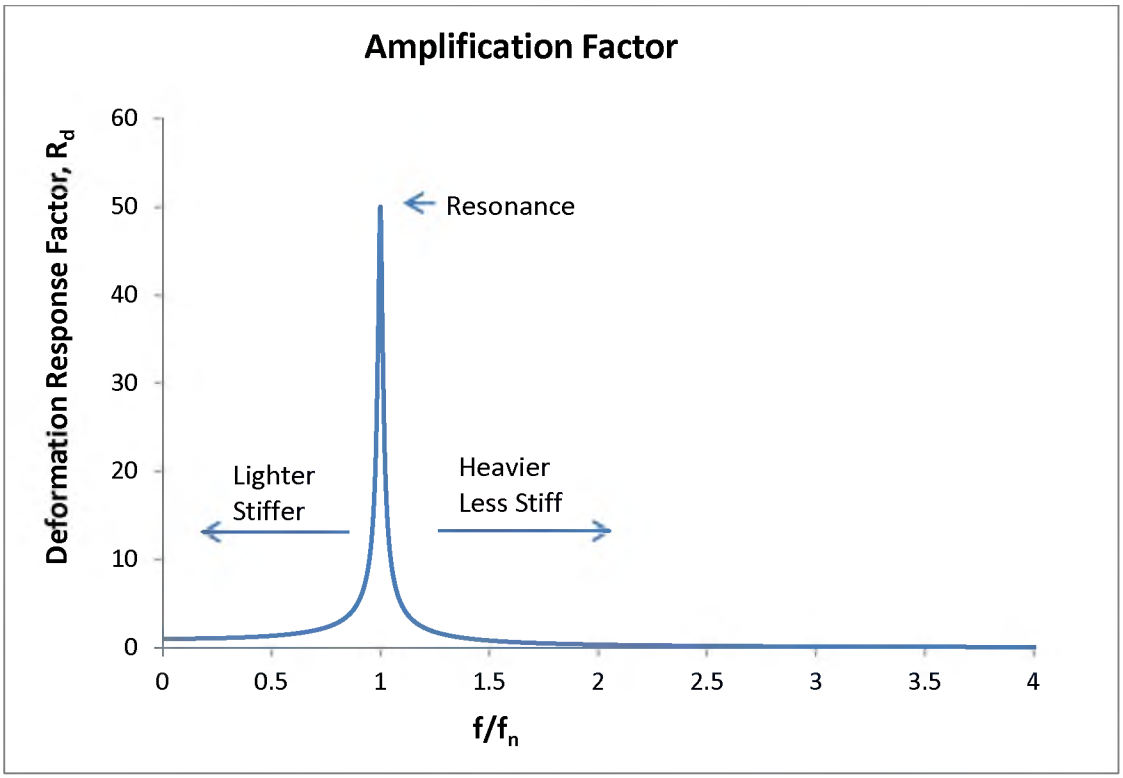

Figure 2.2 – Deformation Amplification Factor

Figure 2.2 shows the effect of f/f_n on the amplification factor. This ratio plays a significant role in the amplification of the static deformation. As the ratio approaches to the unity, amplification factor approaches to the peak. Figure 2.2 shows indirectly the effect of stiffness and mass modifications on the dynamic amplification factor, effects that depend on which side of the peak the frequency ratio is.

Therefore, the actions taken to decrease the amplification factor depend on specific system conditions. For example, if the frequency ratio is less than one (i.e., it is on the left side of the peak in Figure 2.2), the most efficient design solution involves an increase on system stiffness, or a decrease in mass to further reduce the f/f_n ratio

2.3. Transmissibility

There are two cases of vibration transmission that can be evaluated:

i) the force transmitted to the supporting structure, and

ii) the motion of the supporting structure transmitted to the machine. In this research, the harmonic force acting on the system is the force transmitted to the supporting system from the screen. Transmissibility represents the ratio of the amplitude of the force transmitted to the supporting structure to the exciting force.

The transmissibility factor (TR) caused by a harmonic load can be expressed as:

$$TR = \frac{\sqrt{1+(2\xi\omega/\omega_n)^2}}{\sqrt{(1-(\omega/\omega_n)^2)^2+(2\xi\omega/\omega_n)^2}} \qquad (2.12)$$

Figure 2.3 provides a graphical representation of Equation 2.12.

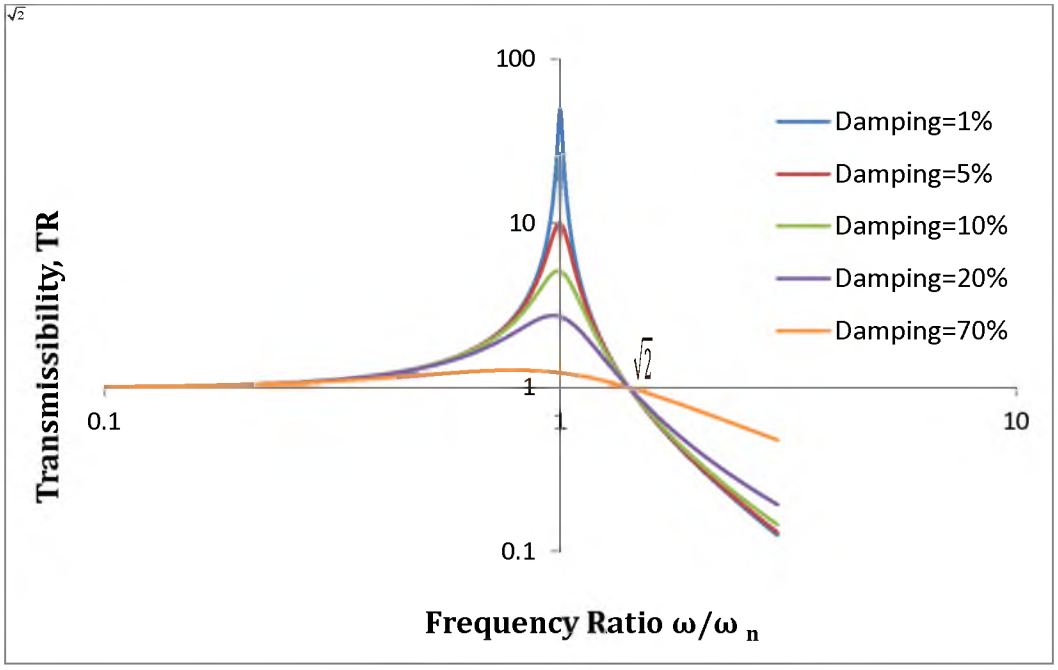

Figure 2.3 – Transmissibility for Harmonic Excitation

As observed, damping reduces the response amplitudes in resonance intervals, but increases the amount of transmitted force to the system for ω/ω_n ratios larger than $\sqrt{2}$.

2.4. System Identification Techniques

2.4.1. Fourier Amplitude Spectrum

The Fourier amplitude spectrum represents the distribution of the amplitude of a dynamic response with respect to frequency. The Fourier spectrum can be used to evaluate the frequency content from recorded time histories. In addition, Fourier analysis is most commonly used to determine the natural frequency of a waveform.

In this study, the Fourier amplitude is used to investigate the amplitude of dynamic response of the screen's supporting structure with varying frequency. The spectrum's peak amplitudes represent the structural flexible modes.

The most common technique to transfer time domain to the frequency domain is called the Fourier Transform. Discrete Fourier Transform (DFT) used in Fourier spectrum analyses requires a discrete input function with a limited duration and it decomposes a set of values into components of different frequencies. Another method to calculate harmonics is using a Fast Fourier Transformation (FFT) algorithm. The FFT algorithm is more efficient and faster than the DFT. The software used in this study to read the data, SeismoSignal, utilizes Fast Fourier Transformation (FFT) to compute the Fourier amplitude spectrum.

2.4.2. Damping

Damping is an effect that reduces the displacement amplitudes in a system. The amplitude of an oscillatory system diminishes due to various mechanisms. In actual structures, these energy dissipating mechanisms include friction between structural and non-structural members, friction at connections, and micro-cracks in concrete, among others. Previous studies on damping values suggest a damping ratio of 1-2% for steel frame

structures (Bentz, 2008). Since the structure investigated is a steel frame with no rigid diaphragms, the damping ratio of 1% was used as first approximation.

The logarithm decrement is a common technique to estimate the percentage of critical damping. The information required from a time history represents a free vibration regime is a time window and the number and amplitude of cycles occurring during that time period:

$$\xi = \frac{1}{2\pi m} \ln \frac{\ddot{u}_n}{\ddot{u}_{n+m}} \tag{2.13}$$

where

ξ: Damping ratio

m: Number of cycles between two amplitudes

n: First amplitude.

3. VIBRATORY MACHINE: SCREEN

3.1. General

The investigated industrial plant uses Rotex Mineral Separator (Screen) to sieve and compact potash material. These mineral separators are designed to meet the screening requirements of minerals applications (Rotex, 2012). The minerals separator maximizes product recoveries at material temperatures up to 400° F (205°C). The separator includes a cam lift rail system for quick screen change capability and sleeveless inlet/outlet connections. Figure 3.1 presents a mineral separator (screen) and its framing system when it sits directly on the ground.

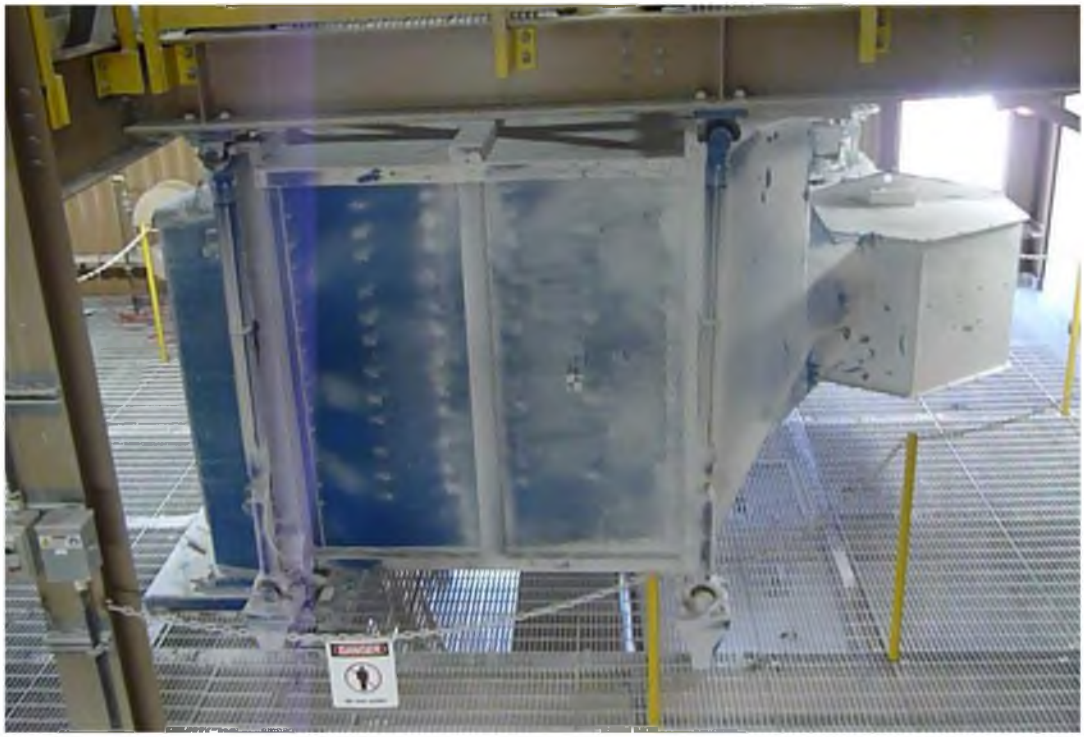

Figure 3.1 – Rotex Mineral Separator

The motion at which the screen starts operations is defined as "patented motion" (Rotex, 2012). This motion is described as "elliptical – linear motion of the minerals separator", providing an efficient screening performance to handle coarse to fine separations from 1/4" to 100 Mesh (6.3mm to 150 µm) through:

- Equal feed distribution to all screen decks.
- Uniform bed depth across entire screen surface.
- Blinding control with durable metal "spring balls" which reduces the risk of fatigue in screen, by the manufacturers.

Structural properties of the Screen are as follows:

According to Rotex (2012), the evaluated screen has the following properties:

- Machine weight empty = 15,700 lbs

- Machine maximum "flooded" weight = Empty weight + (Open volume * Product Density)

$$= 15{,}700\ lbs + (500\ ft^3 * Product\ Density)$$

where

The potash density is $80\ lb/ft^3$. The maximum volume of the screen that can be filled by material is $80\ ft^3$. Thus the maximum machine weight is $22{,}100\ lb$.

The screen has four hangers designated as R1, R2, R3 and R4. Hangers R1 and R2 are closer to the feeder and transfer more static load to the beam than hangers R3 and R4.

Table 3.1 shows the loading the hangers transfer to the supporting frames, as provided by Rotex (2012). The static forces correspond to the weight of the screen; whereas, the dynamic forces represents the loads excited by the screen in horizontal and vertical direction when it is running.

In numerical analysis, for the case when screen was running empty, the static loads shown in Table 3.1 are used as point loads acting on the screen's supporting structure.

Table 3.1 – The Loading Acting on Each Hanger

Hangers	Static Forces (lbs)	Vertical Dynamic Force (lbs)	Horizontal Dynamic Force (lbs)
R1 and R2	5450	± 1800	± 450
R3 and R4	2400	± 1100	± 300

For the screen running with material case, the hanger loads include the static weight of the screen and the material weight. The screen is assumed to be full of material, and the increase in the static forces acting on the hangers is shown in Table 3.2.

According to the fabricator specifications, the screen triggers the following forcing frequencies:

- The machine's operating frequency is 3.43 Hz.
- The machine's vertical dynamic loading occurs at 6.87 Hz ($\omega_{n,v} = 2\pi f_v = 43.16\ rad/s$).
- The machine's horizontal dynamic loading occurs at 3.43 Hz ($\omega_{n,h} = 2\pi f_h = 21.55\ rad/s$).

Table 3.2 – The Weight of Screen and Material Acting on Each Hanger

Hangers	Static Forces (lbs)
R1 and R2	7050
R3 and R4	4000

4. NUMERICAL ANALYSIS

4.1. General

The evaluated screen structure is a 5-story steel tower. The screen is located on the fourth floor of the industrial building. Figure 4.1 shows the fifth floor plan and the points where the screen is attached to the beams. The screen is attached to the upper floor structure by four hangers. The places where the screen is attached to its supporting frame are represented as concentrated loads in Figure 4.1. The vibratory screen is pinned to the supporting structure at the fifth floor, as shown in Figure 4.2.

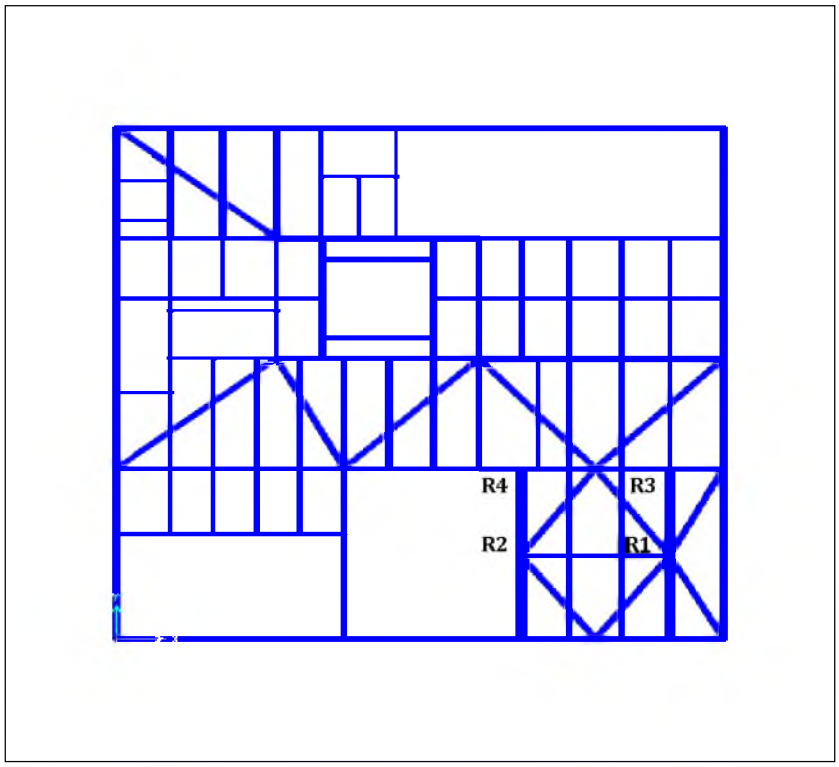

Figure 4.1 – Plan of Fifth Floor and Screen Hangers' Locations

Figure 4.2 – Two Pinned Connections of Screen

The original floor system included a grid of "W" beams that transferred shear forces to the columns, but no bending moment forces. Excessive vertical vibrations of approximately 2.5 in. were reported in the supporting structure because the floor's vertical frequency was very close to the vertical frequency of the system. The vibration was reduced by adding trusses on top of the beams and girders of the support system. The system was evaluated after these modifications had been carried out. In the numerical simulations, the vertical and horizontal dynamic responses of the supporting frame were first investigated separately, and the dynamic response was ultimately combined. Different structural models were created to study the vertical and horizontal motion of the structure. Modal response analysis and acceleration time-history analysis were used in this study.

Modal response analysis can be defined as follows: Mode shapes can be used to determine the system free motion vibration. Under dynamic loading, a structure deflects based on a combination of these modal shapes, which depend only on the mass and stiffness properties. Each mode has its own natural frequency.

The natural vibration period and other frequency modes are obtained from computer based analysis. Modal frequencies can be compared to the forcing frequency generated by the periodic loading. To prevent large dynamic amplifications, the ratio of these two frequencies should not be close to unity.

Acceleration time history analysis can be defines as follows: This system's dynamic response was obtained by defining a periodic function and modeling the structure under this specific periodic loading. Since vibrating screens cause a sinusoidal loading on the supporting structure, it is important to obtain the acceleration and the deflection from time-history analyses. The structural modeling process and the results are discussed in the following two sections.

4.2. Vertical Vibration Response Analysis

There are two phases of structural modeling in this study. The first phase includes a model with a grid of simply supported beams that experiences large dynamic vertical displacement due to vibrations generated by the screen.

The numerical model for the second phase consists of a grid of beams reinforced with a steel truss that modifies the floor frequency.

The sinusoidal force used to model the vertical movement of the screen for both phases is shown in Figure 4.3.

The value of ω in the vertical axis corresponds to the circular vertical forcing frequency of the screen and equals to $\omega_v = 43.16\ rad/s$.

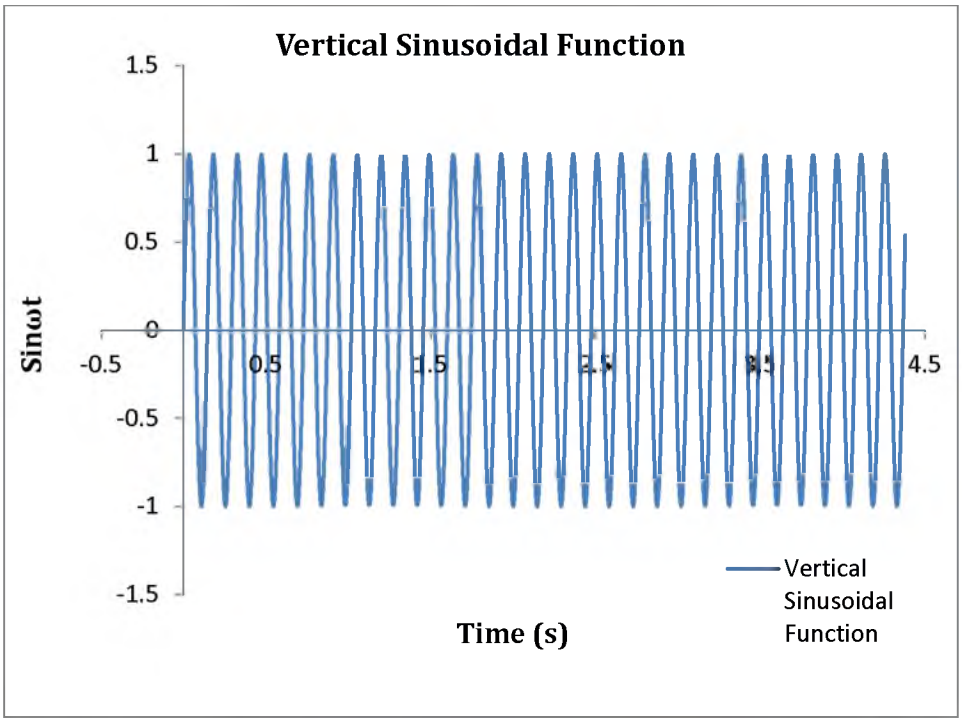

Figure 4.3 – Sinusoidal Function for The Vertical Movement of Screen

4.2.1. First Phase of Analysis

Several structural models were developed in this phase. The first model only includes the beams and girders of the supporting system, and columns are simplified as pin constraints. These pin constraints represent the behavior of bolted beam- column shear connections that transfer no moment.

The screen is hung to the beams at four points. The point loads acting at these four points include the weight of the screen and the material in all structural models. The total screen weight (22,100 lbs) is not distributed evenly. The distribution of total weight (screen and the material) is shown in Figure 4.4. The masses are lumped to the beams where the screen is attached.

The time- history sine function is defined for a period $T = 0.146$ s ($T_v = 1/f_v = 1/6.87Hz$) which represents the vertical forcing period induced by the screen. A time-history function is a good representation of harmonic loading caused by the vibrating

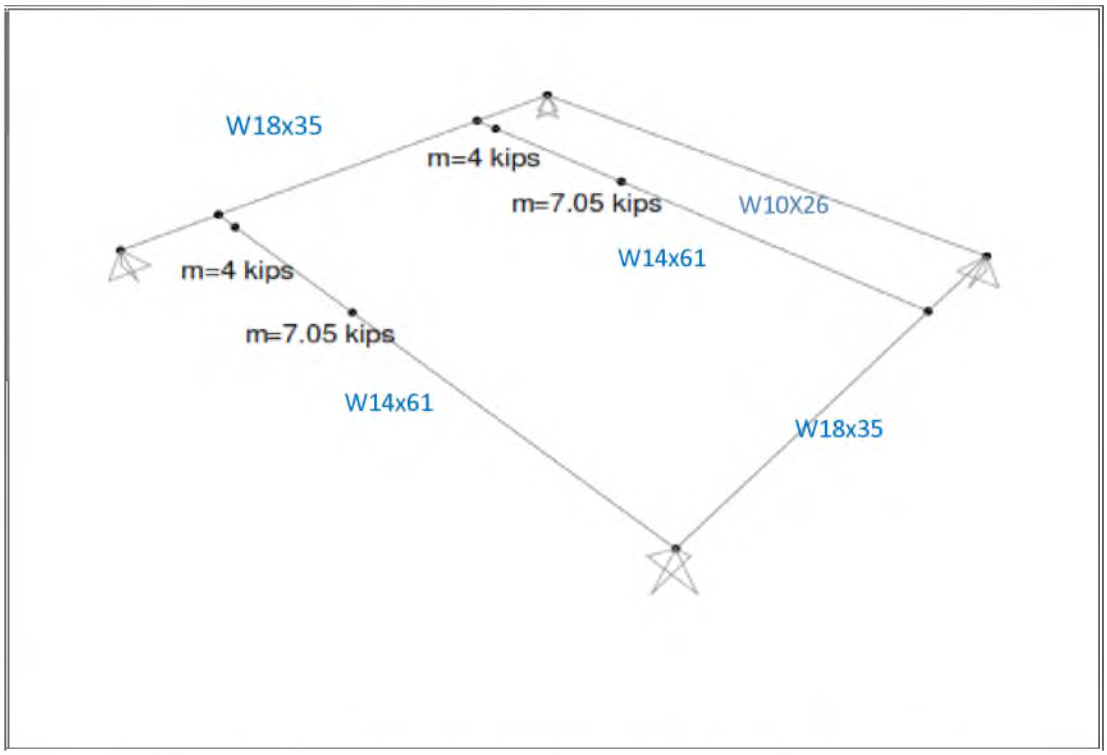

Figure 4.4 –Supporting Structural System with No Columns

machinery. After running the model, the natural frequency ($f_{n,v}$) is calculated as 8.17 Hertz. To avoid amplification of the vertical displacement, the vertical frequency ratio $f_v/f_{n,v}$ should not be close to unity. However, $f_v/f_{n,v} = 6.87/8.17 = 0.84$, a value that ensures significant dynamic amplification. In the second structural model, the columns (W8×31) were added to the model. Since the dynamic properties of the screen remain the same, the same time-history function was used for the second model as well. The natural vertical frequency was calculated as $f_{n,v} = 7.28$ Hz. Including columns in the structural model decreased the natural vertical frequency by 10.8%. The decrease in natural frequency was expected because adding columns to the structural model increases the system's flexibility.

Note that the frequency ratio became closer to the resonance condition $f_v/f_{n,v} = 6.87/7.28 = 0.94$. Figure 4.5 represents the structural model developed for the supporting system of the screen.

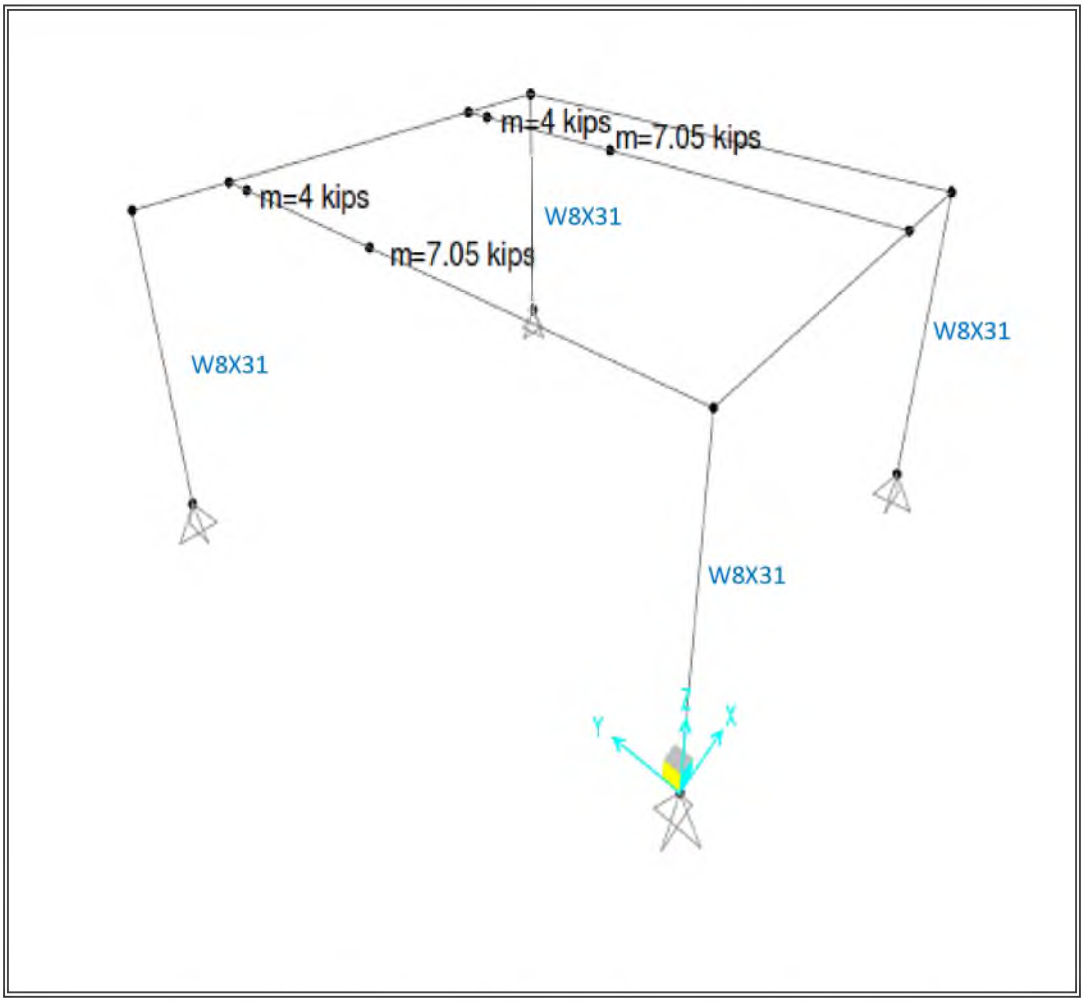

Figure 4.5 – Supporting Structural System with Columns

Based on Equation (2.8), the amplification factors for the two models are 3.5 and 9 (Figure 4.6). The inclusion of columns in the second model, instead of pinned supports, decreased the rigidity of the structural system. Therefore, the amplification factor for the second model was 2.5 times larger than the pinned condition.

In addition, the dynamic response was directly obtained from the computer model by applying a time-history analysis to the frame. The sinusoidal load was applied to the four nodes where the screen is attached. The dynamic displacements at the four nodes were monitored.

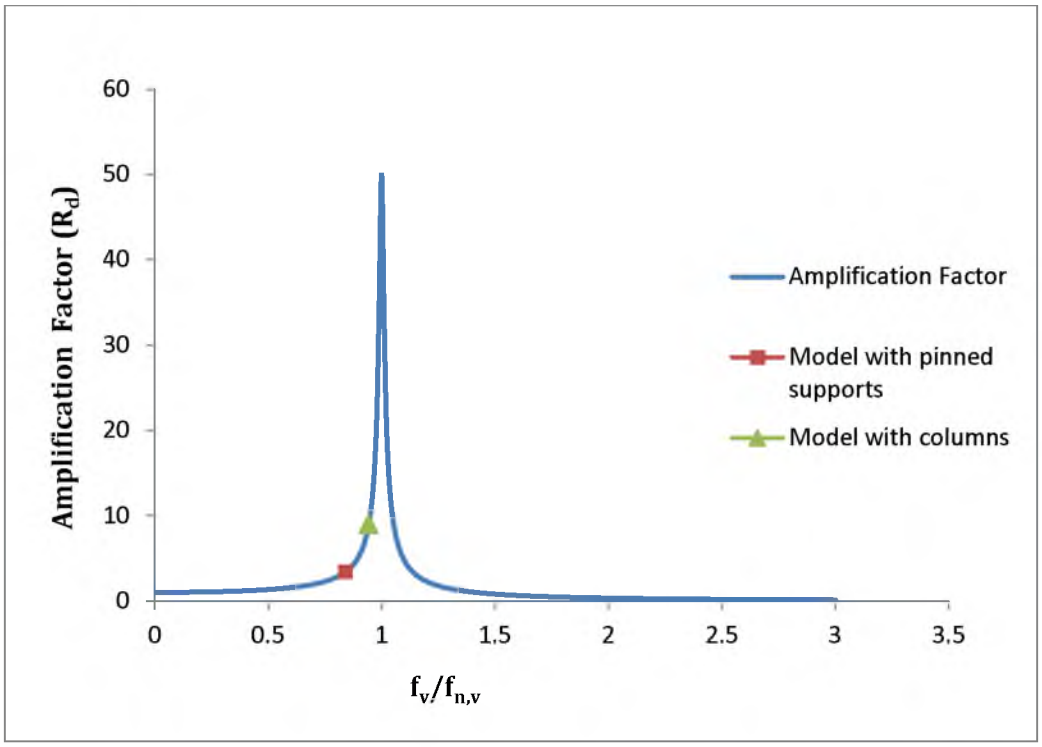

Figure 4.6 – Amplification Factor for First Phase Models

Figure 4.7 shows the time history displacement for node R2 and the maximum dynamic displacement take place at the given node. The maximum displacement is 2.55 in. at node (R2) where the static load is 7.05 kips. The difference with the observed displacement, approximately 2.5 in., is within 1.0%. In addition, Figure 4.8 shows the maximum displacement at node R4, which is approximately 1.66 in. The static load acting on the node is around 4 kips. That is 43% smaller than the load acting on node R2. Therefore, this smaller displacement is expected.

Furthermore, Figures 4.7 and 4.8 shows that the proximity of the natural and forcing frequency triggers a "beating phenomena". When the magnitude of the system and forcing frequencies are close to each other, but not equal, a rapid oscillation with slowly changing amplitude may occur. This situation is known as the "Beating Phenomenon".

Figure 4.7 and 4.8 are good examples of beating action (the variation of amplitude).

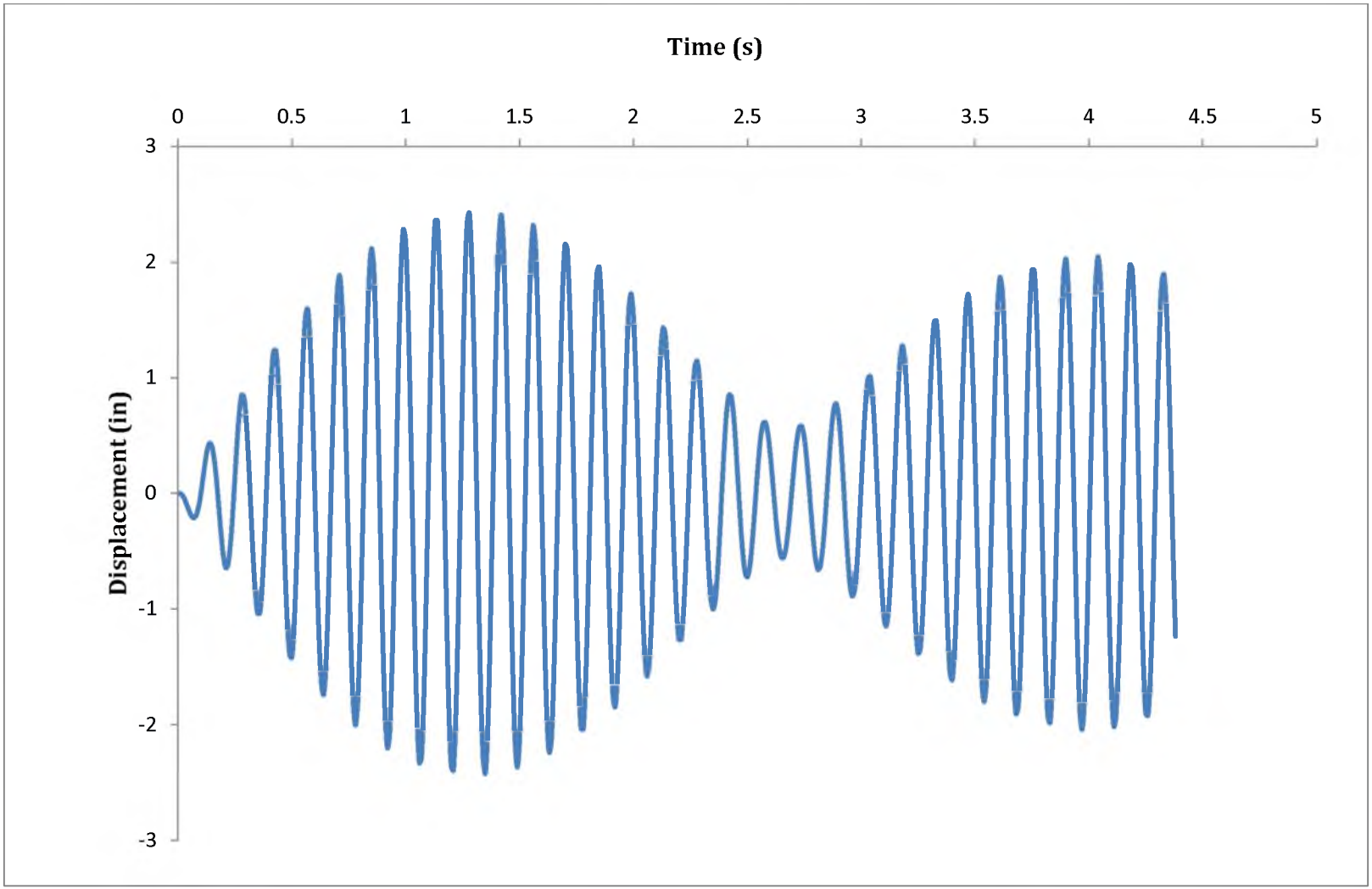

Figure 4.7 – Dynamic Displacement of Node R2

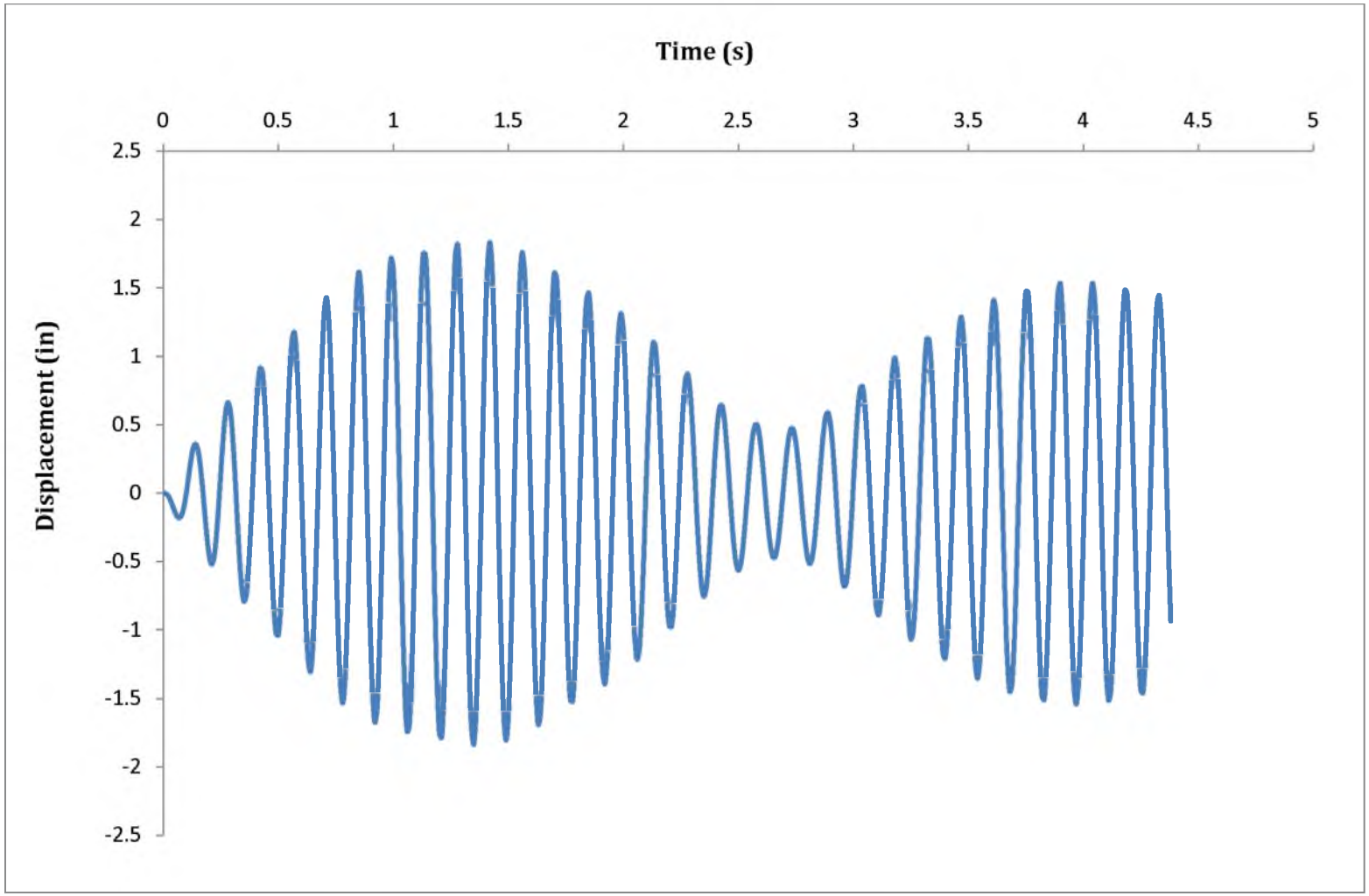

Figure 4.8 – Dynamic Displacement of Node R4

In both models, the natural frequency is very close to the forcing frequency (f) of the screen, which is 6.87 Hertz. This situation causes large structural vibrations and might lead to failure or fatigue. In addition, large vibrations might cause the malfunction of the screen which will lead to productivity problems in the mining facility.

4.2.2. Second Phase Analysis

The structural model in the second phase of the analysis presents a solution to reduce the large vibrations observed in the original building design. The initial design led to large vertical floor vibrations because the natural frequency of the supporting system was close to the forcing frequency of the screen. Therefore, trusses were welded on top of the beams and girders of the supporting system.

This solution resulted in small downtimes, an important advantage given that the mine was in operation. The trusses increased the stiffness of the system, leading to smaller static displacements. More important, the modification resulted in a larger natural frequency of the system, and consequently, a smaller frequency ratio, $f_v/f_{n,v}$. Therefore, the dynamic amplification of the static displacement decreased and excessive vibration in the system was avoided.

Figure 4.9 shows the structural model of the fixed supporting system. Two trusses are connected on the top flange of the beam to which the screen is attached. In addition, there is another truss welded on top flange of the girder. The truss sections are shown in Appendix B. The mass supported by the floor system did not change significantly. However, the natural vertical frequency ($f_{n,v}$) for the modified system is 14.14 Hz. Thus, $f_n/f_{n,v} = 6.87/14.14 = 0.485$, the ratio corresponds to an amplification of 1.31. This frequency ratio is far enough from the unity which prevents excessive vibrations (i.e., $f_v/f_{n,v} = 0.5$). Therefore, the rehab system no longer experiences excessive vibrations.

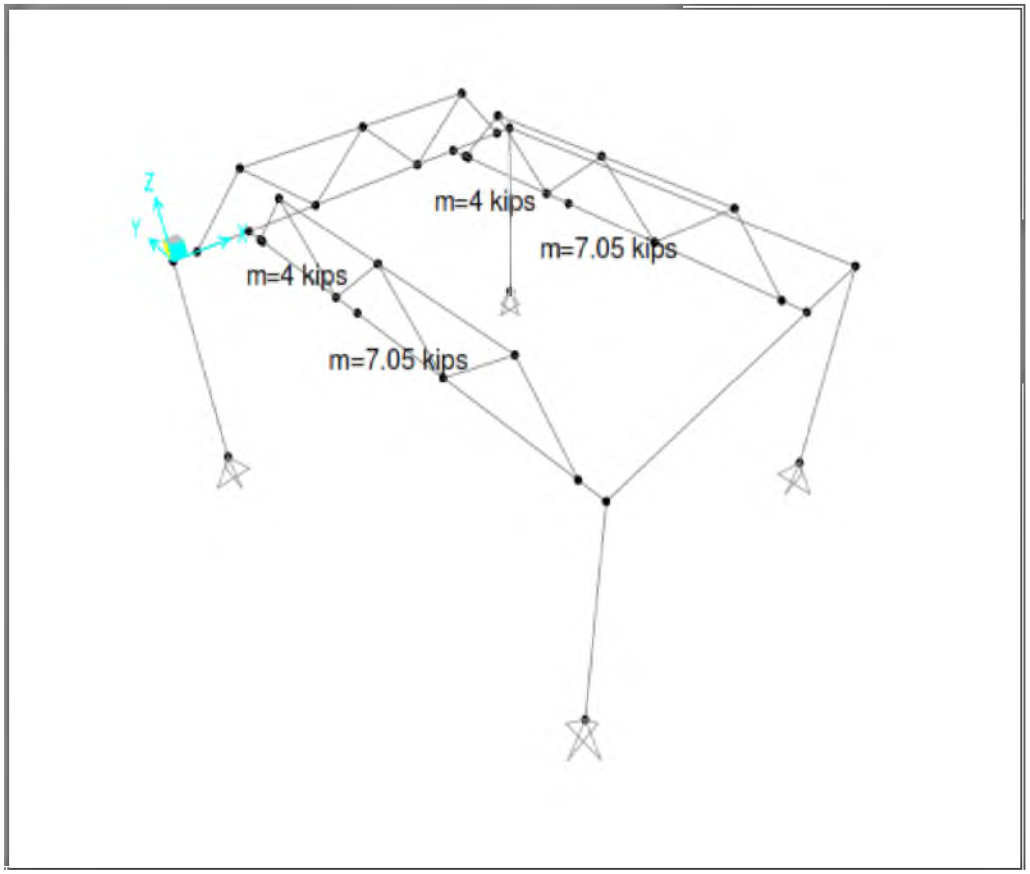

Figure 4.9 – Supporting Structural System with Additional Truss Fixes

In addition, time- history analysis shows the dynamic displacements at the nodes where the screen is attached.

Figure 4.10 and 4.11 show the displacements at nodes R2 and R4. After adding trusses in the structural model, the maximum dynamic displacement at node R2 is 0.07 in., which is a decrease of 97.2 % in dynamic displacements.

Figure 4.11 shows that the displacement at node R4 is decreased from 1.66 in. to 0.04 in. after the insertion of trusses. The beating phenomenon exhibited by the original model is no longer present in the dynamic response because the frequency ratio is not close to the unity. The response time history also shows the transient component of the dynamic response during the first 2 s.

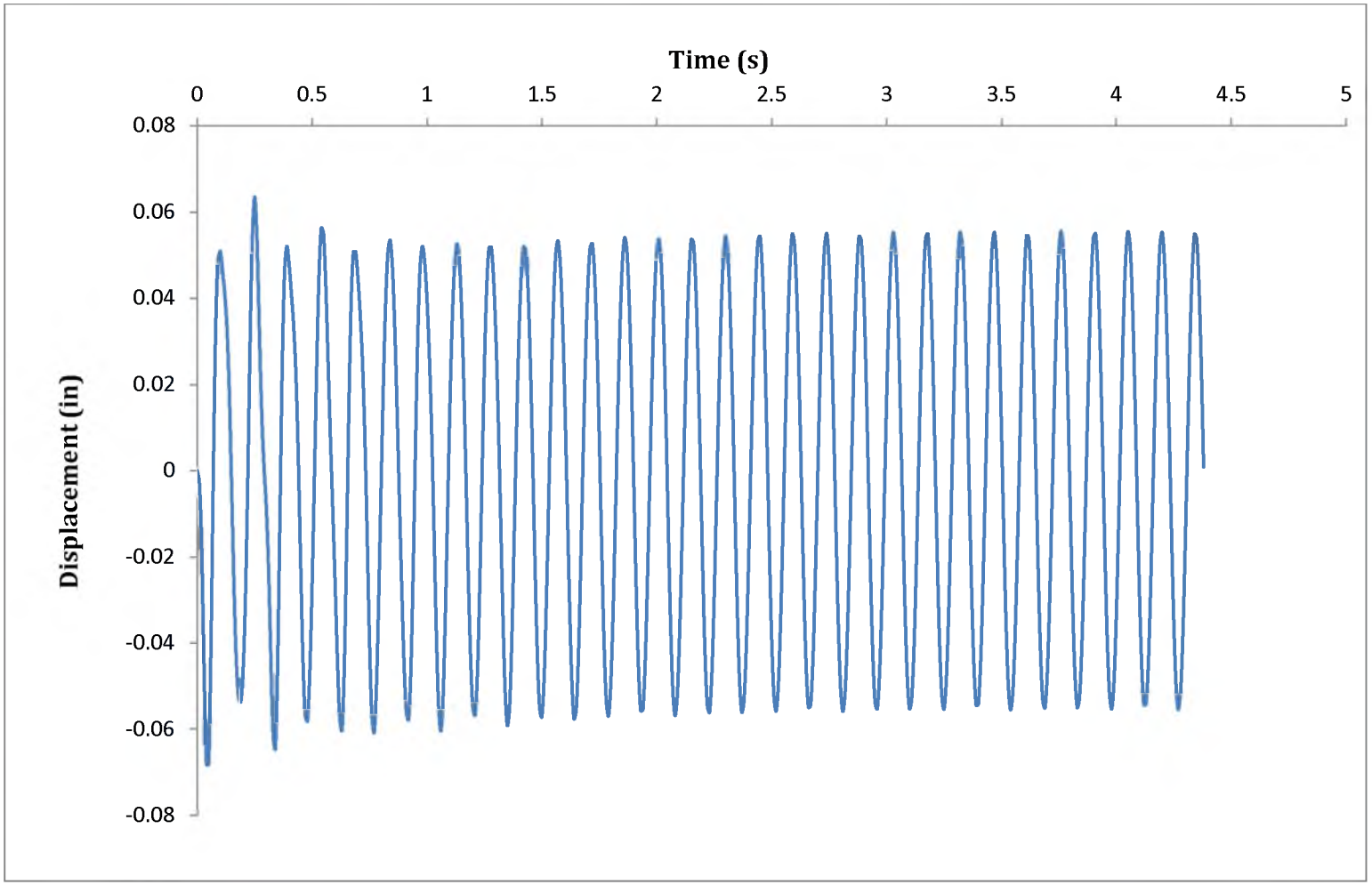

Figure 4.10 – Dynamic Displacement of Node R2 (with Trusses)

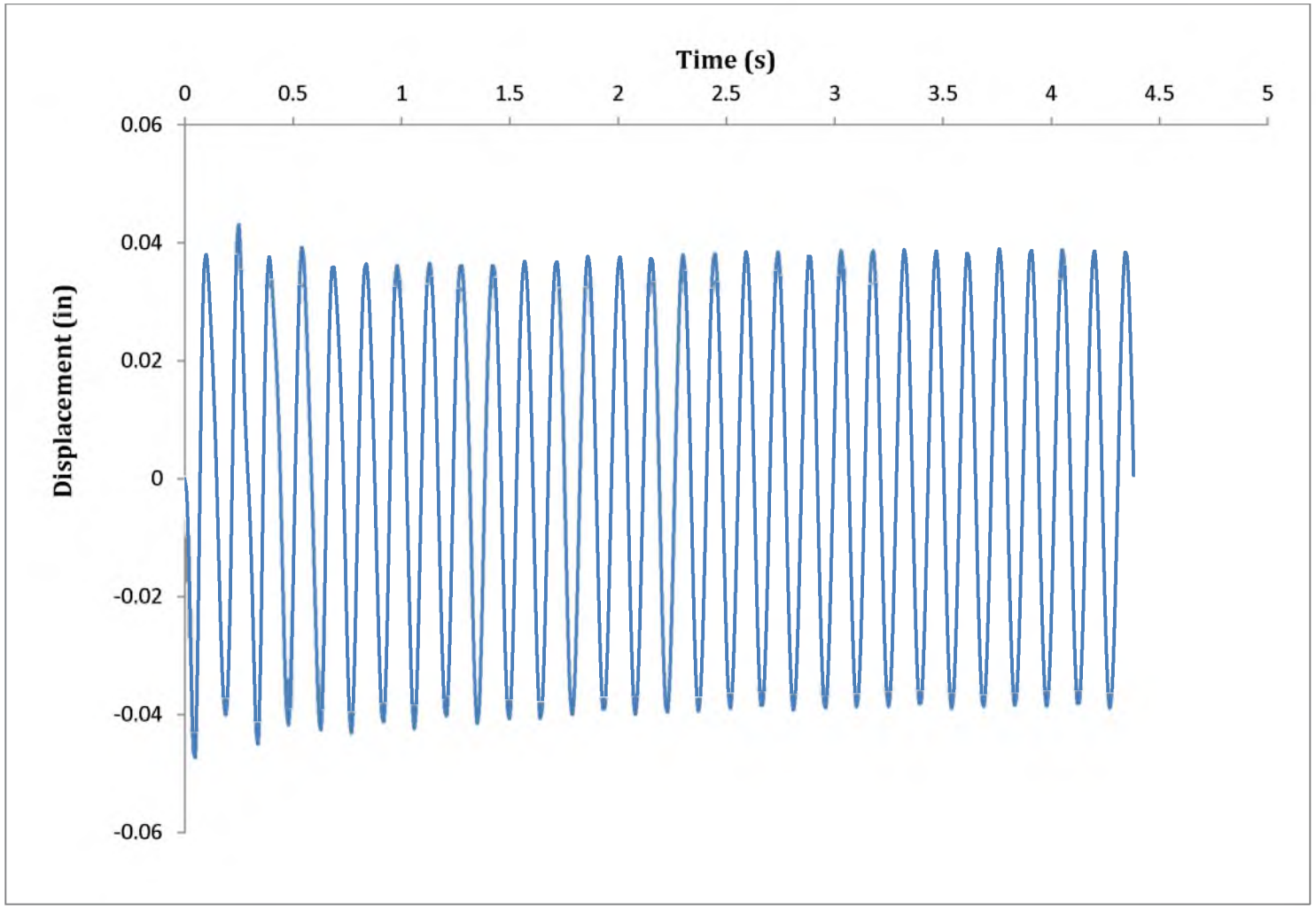

Figure 4.11 – Dynamic Displacements of Node R4 (with Trusses)

Table 4.1 and 4.2 show the summary of results calculated in numerical analyses. They consist of both first phase and second phase analyses for vertical vibration. They include the frequencies obtained from modal analysis and the displacements from acceleration time history analysis.

The vertical analyses results will be discussed in detailed in Chapter 6. The comparison of the numerical and experimental results will be discussed in Chapter 7.

Table 4.1– Summary of Numerical Analysis Results for Empty Case

Empty Case	Vertical Frequency, $f_{n,v}$	Period, T_v	Vertical Displacement, δ_v
System without trusses	8.33 Hz	0.120 s	1.00 in
System with trusses	15.40 Hz	0.064 s	0.06 in

Table 4.2 – Summary of Numerical Analysis Results for Screen Running with Material

Full Case	Vertical Frequency, $f_{n,v}$	Period, T_v	Vertical Displacement, δ_v
System without trusses	7.28 Hz	0.137 s	2.55 in
System with trusses	14.14 Hz	0.071 s	0.07 in

4.3. Horizontal Vibration Response Analysis

For modeling the horizontal vibration, a tri-dimensional frame was created in SAP2000 to obtain a good approximation of the natural horizontal frequency. Figure 4.12 shows the structural model used for horizontal vibration analysis. The structural members such as vertical bracings, horizontal bracings, beams, and girders participate in the natural horizontal frequency. Vertical bracings decrease the sway of the structure under horizontal loading, by increasing the building's lateral stiffness and natural frequency.

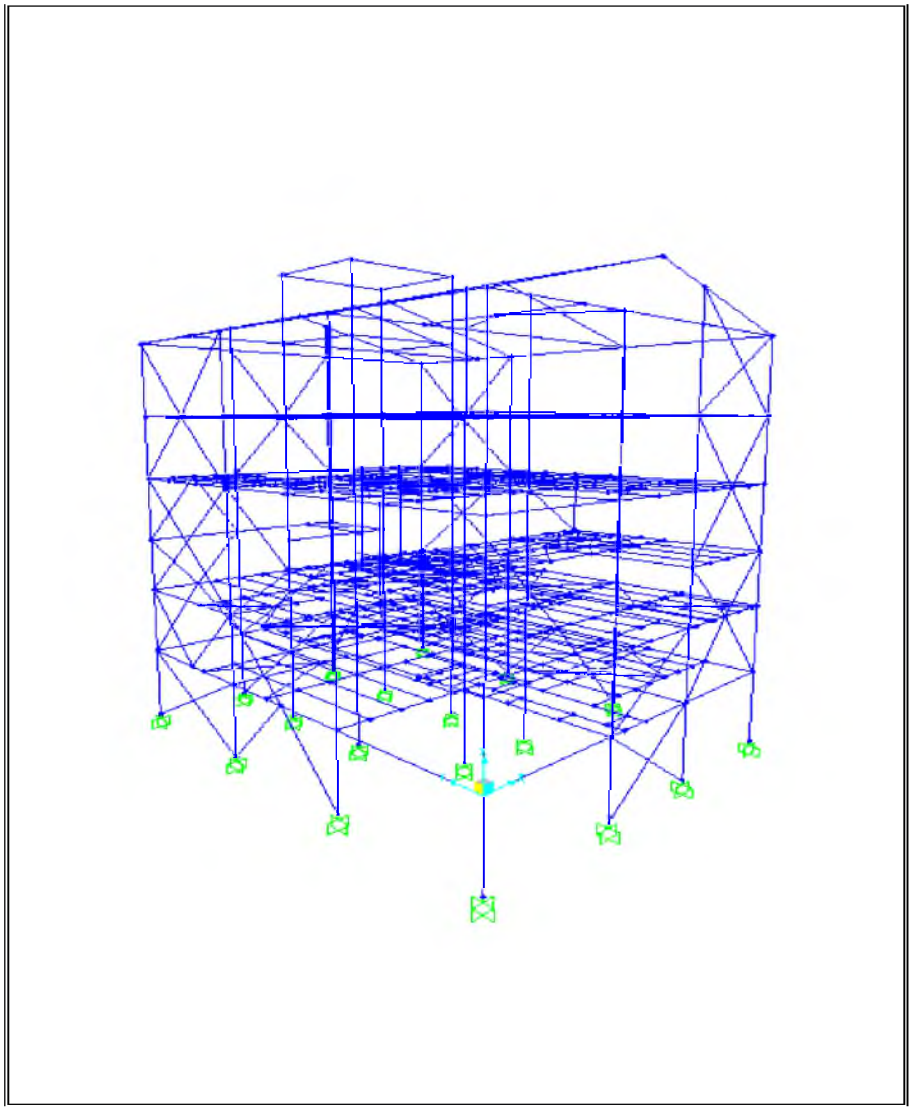

Figure 4.12 – Screen Tower

Horizontal bracings also reduce the floor horizontal displacements. To avoid significant dynamic amplification of the horizontal displacement, the frequency ratio should not be close to unity. That is, the natural horizontal frequency of the structure should not be close to horizontal forcing frequency of 3.43 Hz.

The time-history function is defined for the horizontal frequency of the screen. The sinusoidal force generated by the horizontal movement of the screen is defined as shown in Figure 4.13. In Figure 4.13, the screen's horizontal frequency is $\omega = 21.55\ rad/s$. In addition to the screen's weight, the siding and the bar grating on the floors were included in the design as distributed dead loads. The distributed load for siding was taken as 5 psf.

The size of serrated bar grating used for slabs was 1 ¼×3/16", and the distributed weight of the gratings was assumed as 9 psf. A total of 14 psf distributed load was applied to the main beams and girders of the structure.

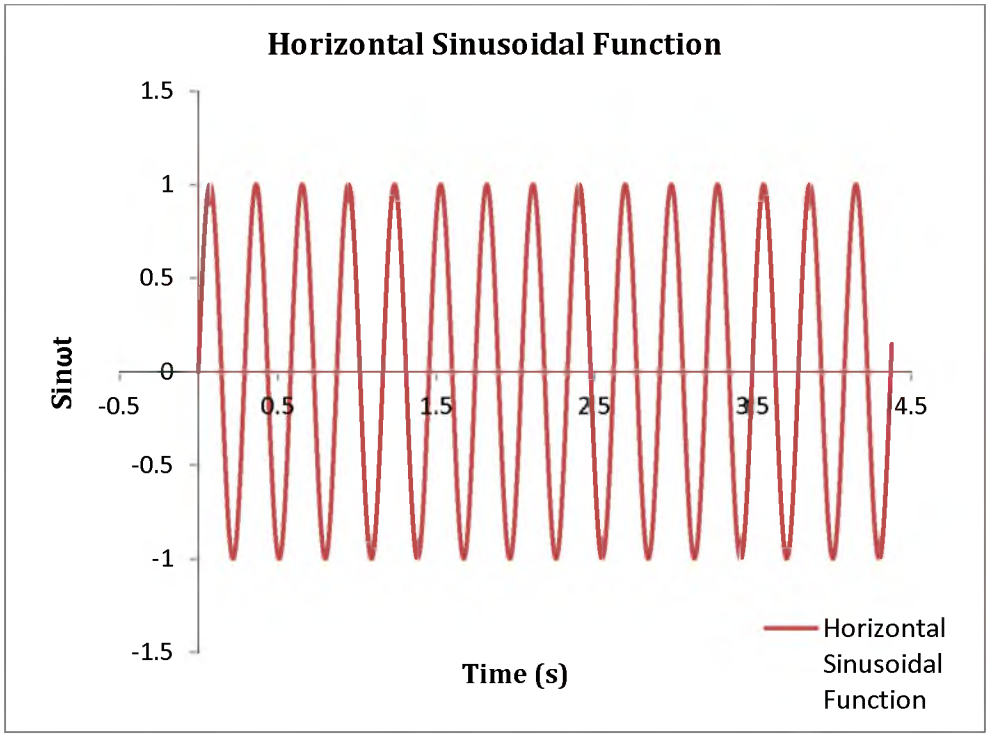

Figure 4.13- Sinusoidal Function for The Horizontal Movement of Screen

There were two cases investigated in this section. The horizontal natural frequency of the tower was calculated for the screen running empty and with material. However, the horizontal natural frequency obtained from the structural model was practically the same for both cases. The horizontal frequencies in x- and y- directions are $f_{n,x} = 1.92$ Hz and $f_{n,y} = 2.07$ Hz, respectively. These horizontal frequencies differ 7.25% and the ratios are as follows; $f_h/f_{n,x} = 3.43/1.92 = 1.78$ and $f_h/f_{n,y} = 3.43/2.07 = 1.66$. These frequency ratios correspond to dynamic amplification factors of 0.35 and 0.57 for x- and y-directions, respectively, assuming an SDOF system subjected to harmonic excitations (Figure 4.14).

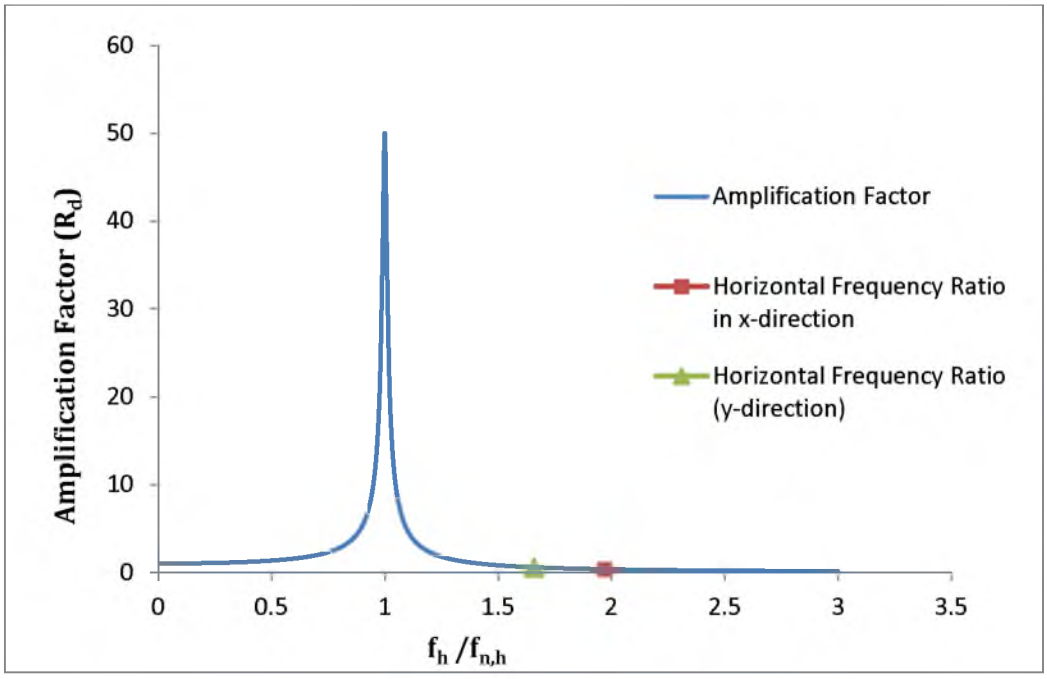

Figure 4.14 – Amplification Factor for Horizontal Vibration

5. FIELD EXPERIMENTS

5.1. General

Field investigations were carried out at the industrial plant to validate the numerical results. The following three cases were investigated during the field experiments.

i. Ambient vibration, when all machineries in mine are in rest

ii. Harmonic vibration with the screen running empty

iii. Harmonic vibration with the screen running with material.

Accelerometers with data acquisition system were used to perform the field experiments. The devices were bolted to several critical locations on the supporting frame of the screen on the fifth floor. Figure 5.1 shows the location where the readings were recorded in the structural model and Figure 5.2 shows a picture of the recording location.

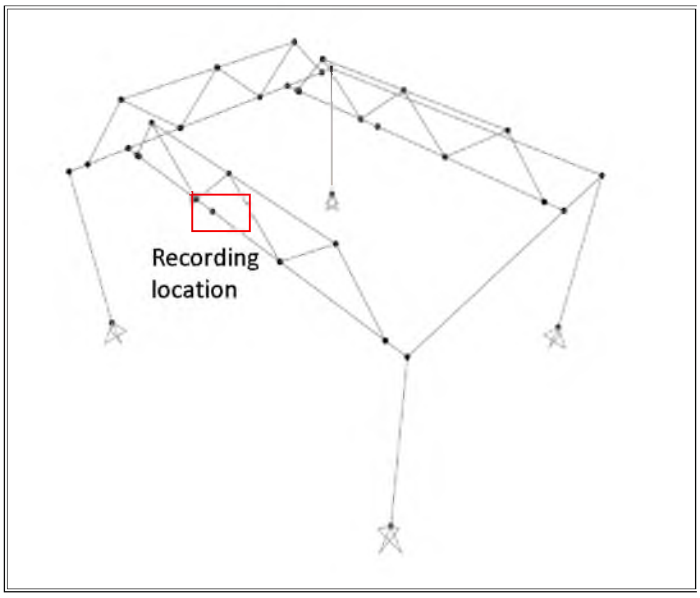

Figure 5.1 – The Location Where The Readings Are Recorded

Figure 5.2 – Recording Location

Two visits were made to the plant. In the first visit, seven recording sessions were carried out to obtain the ambient vibration and harmonic vibration with empty screen responses. In the second visit, the screen was in operation and two different recording sessions were carried out.

5.1.1. Ambient Vibration

The first reading was recorded when the screen was at rest to identify the parameters controlling the dynamic response under small amplitudes. This data is relevant because it provides an approximation of the system natural frequencies. The first recording, CN009, represents the ambient case. This recording is used for interpretation of the data from the field experiments. The accelerometers recorded the acceleration time histories in the three directions. CN009.XYO refers to the record x- direction. Figure 5.3 and 5.4 show the acceleration-time history and velocity-time history for x-direction, respectively. Table 5.1 represents the baseline correction and filtering used for this case. Appendix B addresses the filtering types and baseline correction.

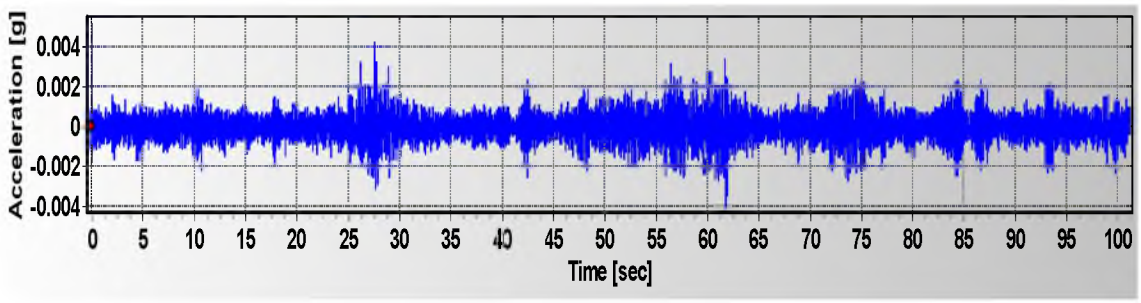

Figure 5.3 – Acceleration Time History for Ambient Case

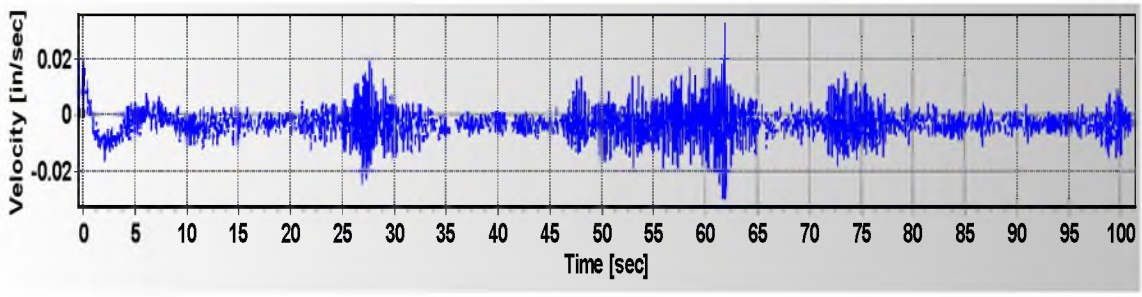

Figure 5.4 – Velocity Time History for Ambient Case

Table 5.1 – Baseline Correction and Filtering for CN009-XYO

Baseline Correction	Filtering				
Polynomial Type	Filter Type	Filter Configuration	Order	Freq 1	Freq 2
Linear	Butterworth	Bandpass	4th	0.10 Hz	45 Hz

The maximum absolute acceleration and the maximum velocity for the ambient case is 0.005 g and 0.033 in/s in x-direction. The maximum displacement derived from the acceleration time history was 0.012 in.

The Fourier amplitude is shown in Figure 5.5 for this specific case. The peak frequency, corresponding to natural frequency of the system, obtained from Fourier amplitude is $f_{n,x} = 2.14$ Hz which corresponds to a period $T_{n,x} = 0.467$ s. The peak at 5.28 Hz is the harmonic reflection of the other peaks at 1.80 and 3.56 Hz.

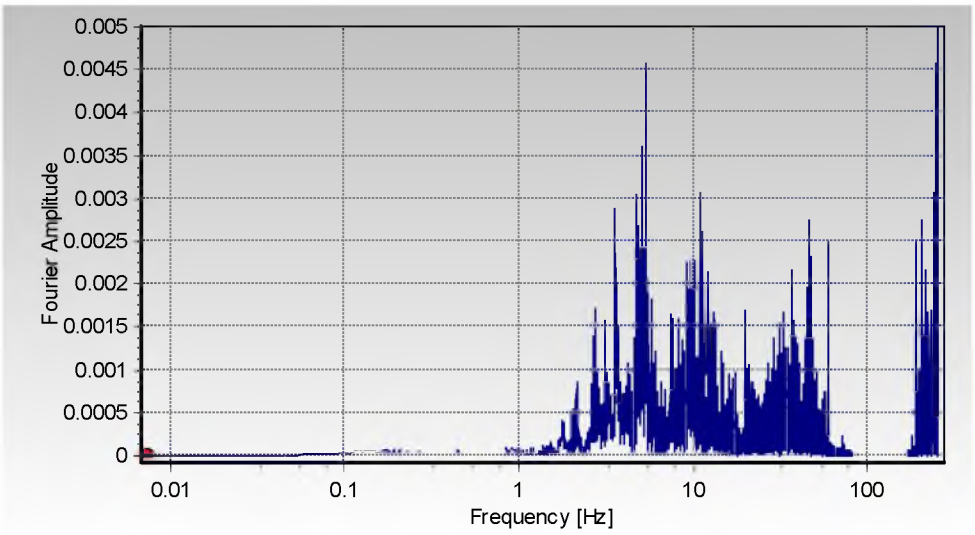

Figure 5.5 – Fourier Spectrum of CN009.XYO

The recording corresponding to the orthogonal horizontal direction, y-direction is CN009.XY1. Baseline correction and filtering shown in Table 5.1 is also used for CN009.XY1.The acceleration and velocity time histories for the ambient case in y- direction are shown in Figure 5.6 and 5.7, respectively.

The maximum absolute acceleration and the maximum absolute velocity were 0.005 g and 0.045 in/s. The maximum displacement was 0.012 in. The fundamental frequency in y- direction is $f_{n,y} = 2.04$ Hz corresponding to a period of $T_{n,y} = 0.490$ s. The Fourier amplitude in y- direction is shown in Figure 5.8.

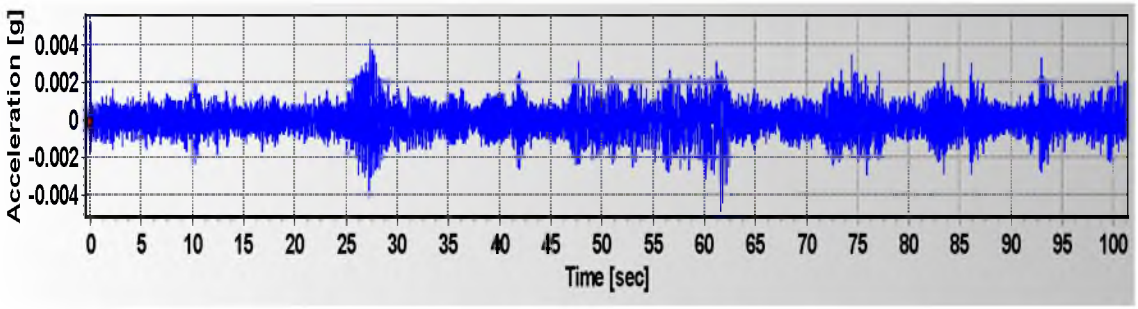

Figure 5.6 – Acceleration Time History for CN009.XY1

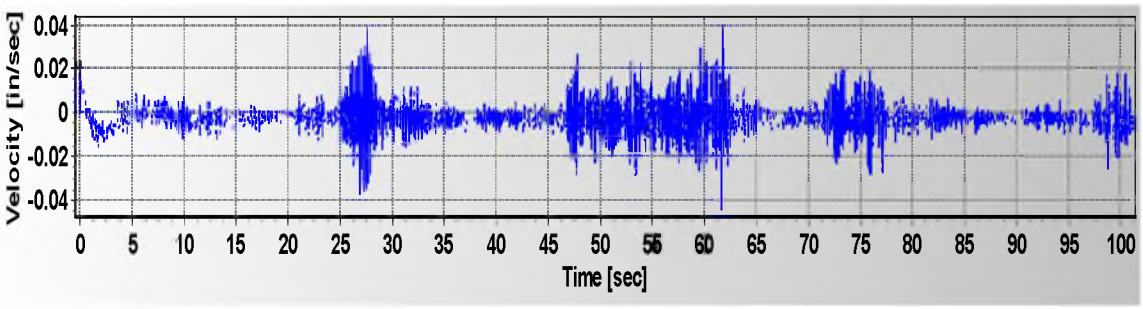

Figure 5.7 – Velocity Time History for CN009.XY1

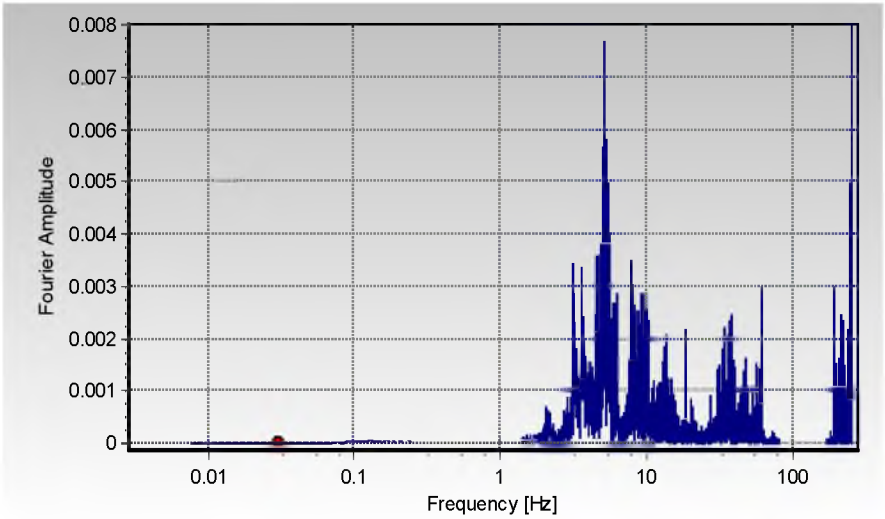

Figure 5.8 – Fourier Spectrum of CN009.XY1

The recording corresponding to the vertical response of the supporting frame is CN009. XY2. The same filter and baseline correction of Table 5.1 is applied to the data. The maximum absolute acceleration and the velocity in vertical direction is 0.005 g and 0.028 in/s. The maximum displacement was calculated as 0.002 in. Figure 5.9 represents the acceleration time history in z-direction; whereas Figure 5.10 shows the velocity time history values. The Fourier spectrum for vertical direction is shown in Figure 5.11. The peak frequency is $f_{n,v} = 9.38$ Hz, equivalent to a period $T_{n,v} = 0.107$ s.

The data obtained from the ambient case provides the ability to calibrate the data of recording of harmonic vibrations with the screen running empty and with material.

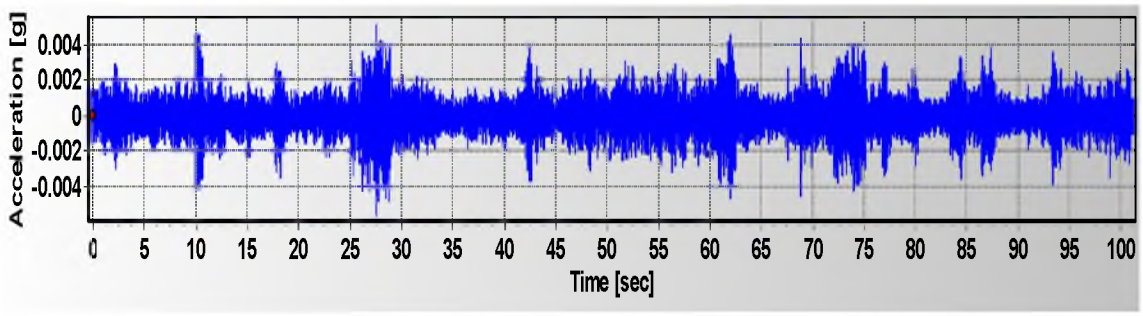

Figure 5.9 – The Acceleration Time History of CN009-XY2

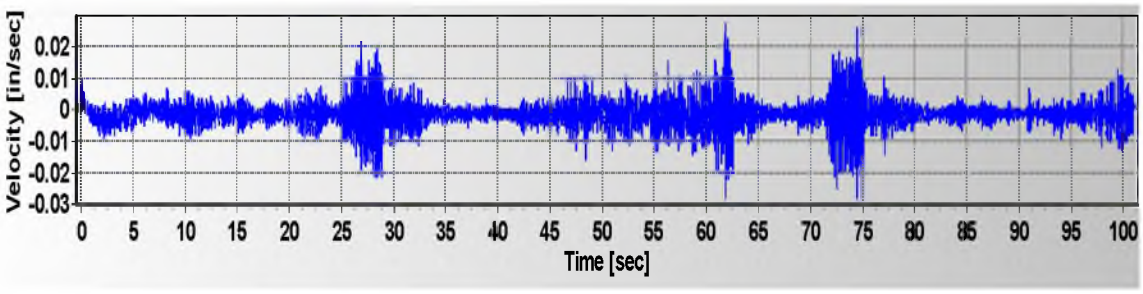

Figure 5.10 – The Velocity Time History of CN009-XY2

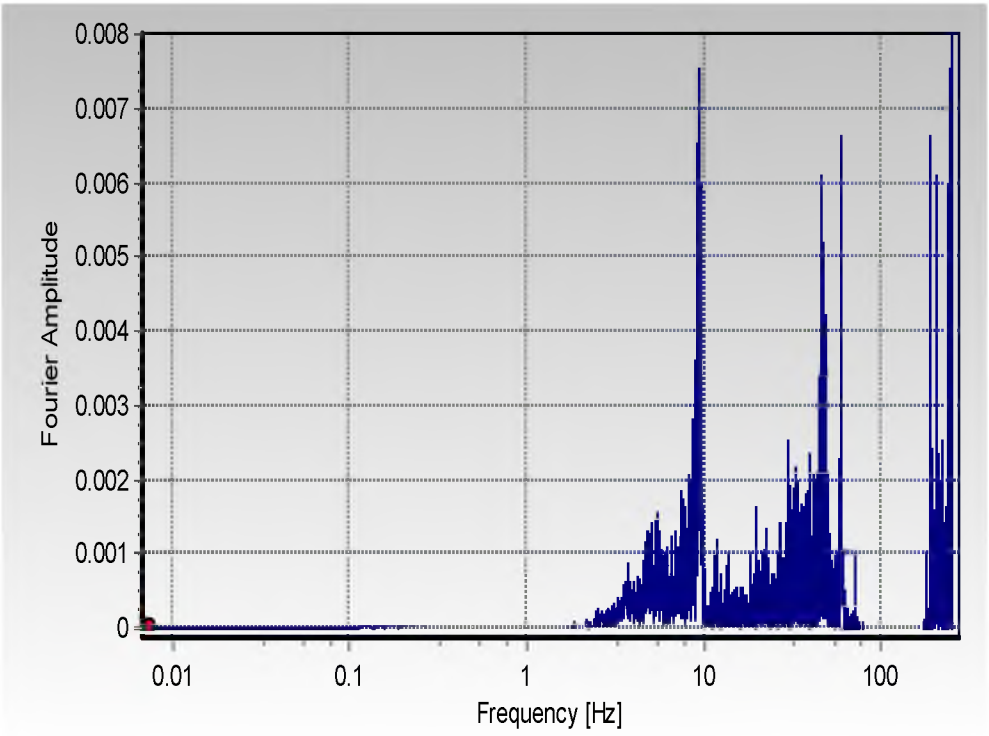

Figure 5.11 – The Fourier Spectrum of CN009.XY2

5.1.2. Harmonic Vibrations with the Screen Running Empty

The readings for harmonic loads of the empty screen were recorded at the same location as the ambient case. The second recording, CN010, represents the screen running without material.

This experimental phase included 40 seconds of ambient vibration before the screen was started to record the dynamic transient response. The recording corresponds to the vibrations in x-direction is CN010.

Figure 5.12 shows the acceleration time history for the first 100 seconds of recording, including the start of the operation period at about 34 seconds. At first, a higher range of frequency filtering is used for the CN010.XYO recording. The specific information related to the baseline correction and filtering used is shown in Table 5.2.

The maximum absolute acceleration was 0.06 g due to the high frequency filtering. However, when the value of frequency 2 in Table 5.2 was changed to the lower frequency of 45 Hz, the maximum absolute acceleration decreased to 0.037 g. This indicates that the larger accelerations are triggered by very high frequencies.

On the other hand, narrowing down the frequency range did not affect the maximum absolute velocity of the system. The maximum absolute velocity was about 0.14 in/s and the maximum displacement was calculated as 0.015 in.

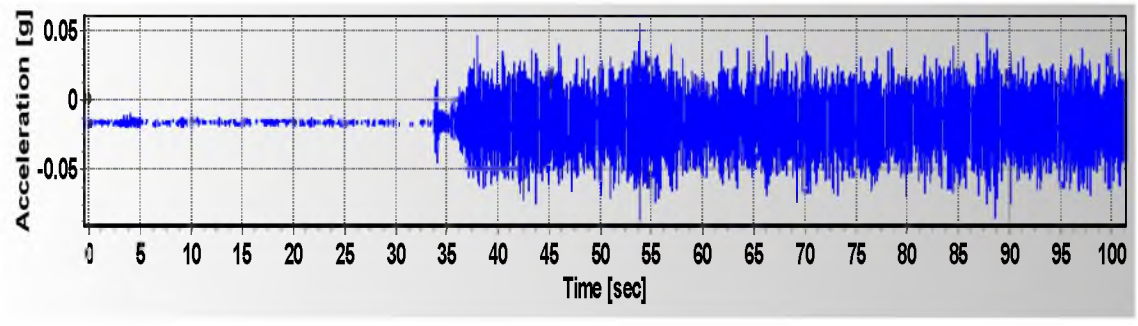

Figure 5.12 – Acceleration Time History of CN010.XY0

Table 5.2 – Baseline Correction and Filtering for CN010-XYO

Baseline Correction	Filtering				
Polynomial Type	Filter Type	Filter Configuration	Order	Freq 1	Freq 2
Linear	Butterworth	Bandpass	4th	0.10 Hz	95

The narrower band of frequency filtering is used for the rest of the recordings because the higher frequencies most likely correspond to the noises or other unrelated parameters. Table 5.1 shows the filtering and baseline correction used.

Figure 5.13 shows the Fourier spectrum of the system for x-direction. The spectrum shows the peak frequency of 3.43 Hz (T = 0.292 s) and 6.9 Hz (0.145 s). The former one represents the screen's horizontal frequency, whereas the latter corresponds to its vertical frequency.

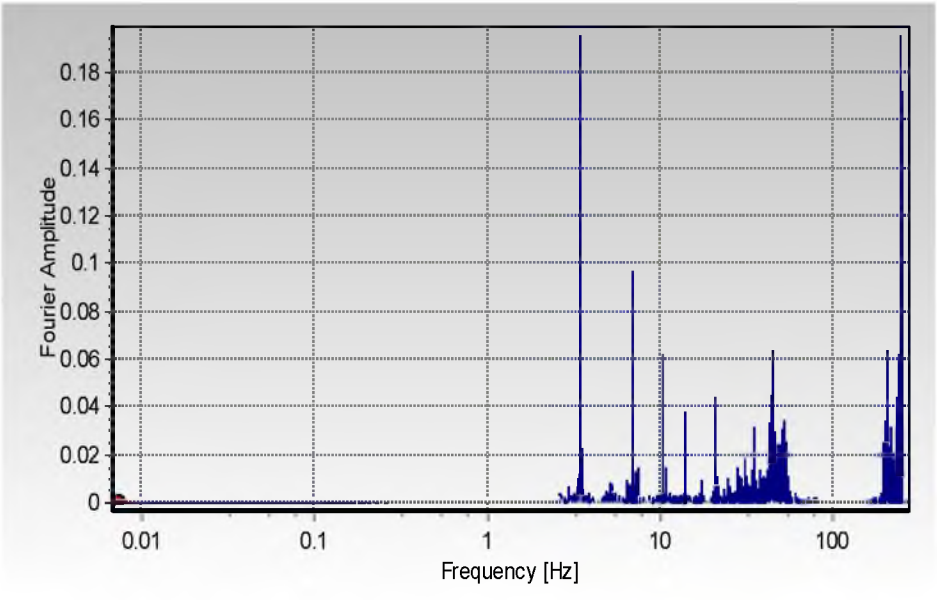

Figure 5.13 – Fourier Spectrum of CN010.XYO

The recording, CN010.XY1, represents the motion in y-direction for the first 100 seconds of the acceleration and velocity time histories (Figures 5.14 and 5.15, respectively). The maximum absolute acceleration and velocity is 0.038 g and is 0.130 in/s. The maximum displacement is calculated as 0.016 in.

The Fourier spectrum for y-horizontal direction shows two significant peak values at the screen's horizontal and vertical frequency. The peak for natural horizontal frequency is much smaller than the peaks for the screen's forcing frequencies due to the intensity of screen's periodic movement at that specific recording location. The peak horizontal natural frequency is 2.16 Hz. It is seen more clearly in the ambient case. In addition, there is also a peak at a frequency of 13.8 Hz. The Fourier spectrum is shown in Figure 5.16 for CN010.XY1.

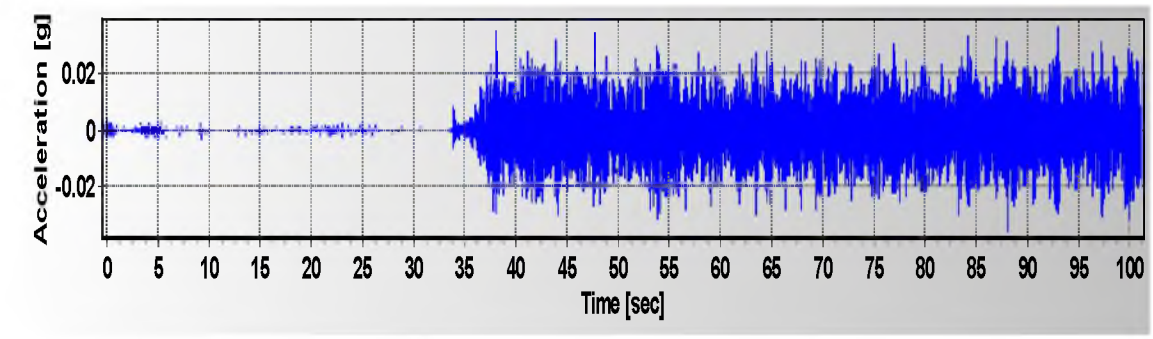

Figure 5.14- The Acceleration Time History of CN010.XY1

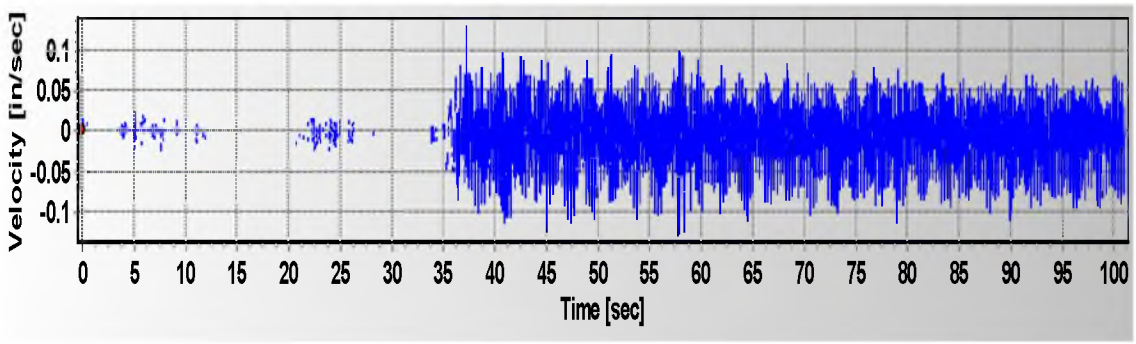

Figure 5.15 – The Velocity Time History of CN010.XY1

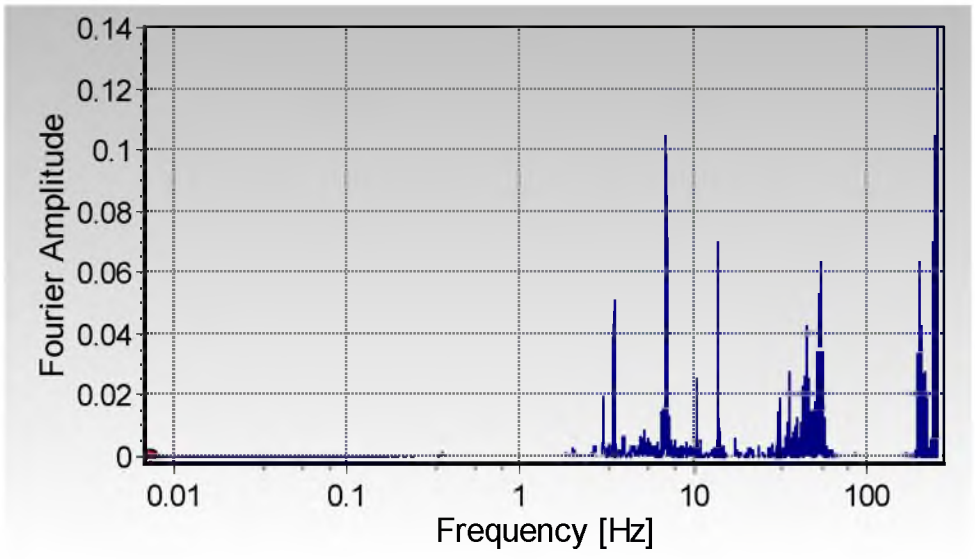

Figure 5.16 – Fourier Spectrum of CN010.XY1

The vertical recording for the empty case is CN010.XY2 and Figure 5.17 represents the acceleration-time history filtered accordingly to the data given in Table 5.1. The maximum vertical acceleration and velocity obtained from the experiments are 0.133 g and 0.35 in/s. The maximum displacement is calculated as 0.06 in.

The Fourier spectrum for vertical case is shown in Figure 5.18. Apart from the screen's operating horizontal and vertical frequencies, there is a peak frequency of 2.18 Hz and 13.8 Hz.

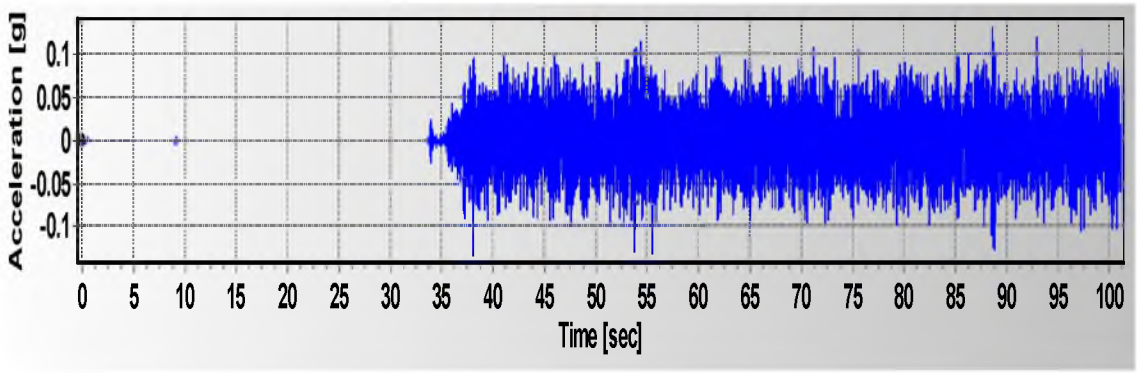

Figure 5.17 – Acceleration Time History of CN010-XY2

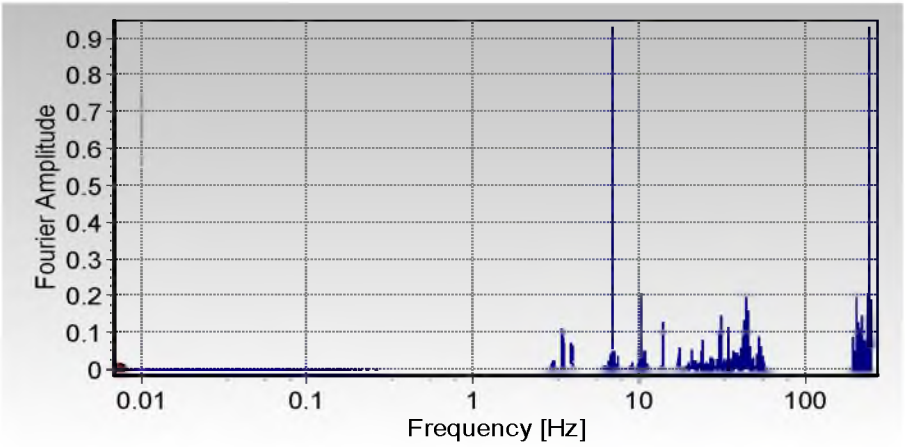

Figure 5.18 – Fourier Spectrum of CN010.XY2

In addition, the data from CN010.XY2 are also used to calculate the damping of the system. The damping ratio of the evaluated steel building is calculated by using the data obtained from field experiments. Figure 5.19 represents the acceleration time history (ATH) after the screen has stopped.

Damping can be approximately calculated as follows: To estimate the percentage of critical damping, a time widow was selected in the ATH of Figure 5.19, from 35.196 s. to 35.216 s. A single cycle was identified in this time window. Using Equation 2.13, the damping ratio of the structure was calculated as 0.97% for the values:

$\ddot{u}_n = 0.02031g$

$\ddot{u}_{n+m} = 0.01911g$

$m = 1$ Cycle

Figure 5.20 shows the two acceleration amplitudes used to calculate the damping ratio of the system. The obtained damping ratio is an approximate value because the dampening of the screen's motion when it is shut down is not rigorously a free vibration regime. Based on damping ratio calculations obtained by field measurements, the damping ratio is taken as 1% in numerical analyses.

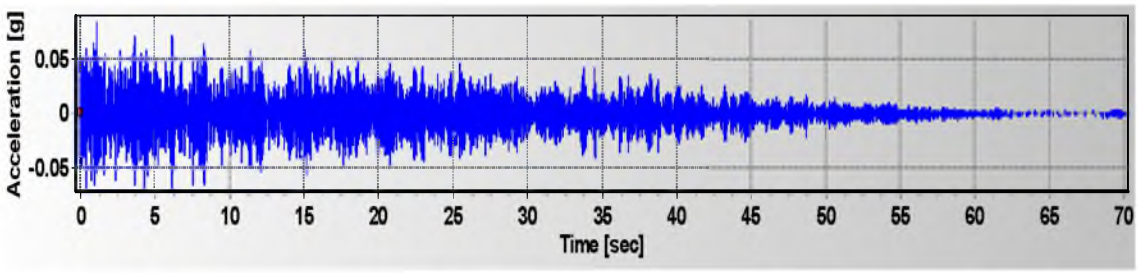

Figure 5.19 – Acceleration Time History of Free Vibration (CN010.XY2)

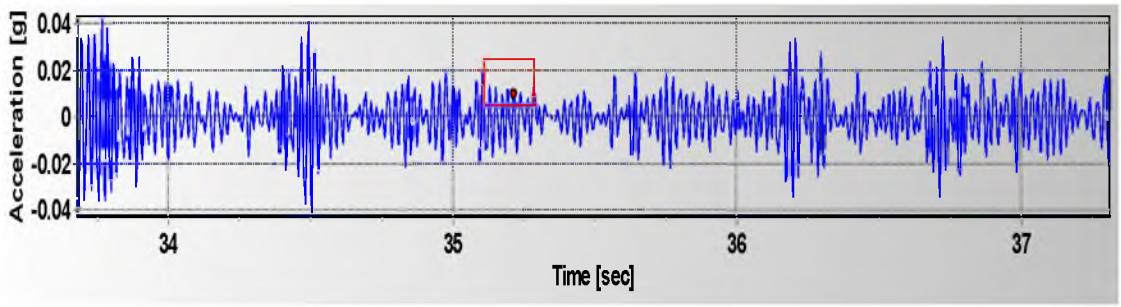

Figure 5.20 – Two Amplitudes Used for Damping Ratio of The System

5.1.3. Harmonic Vibrations with the Screen Running with Material

A second visit to the mine included recordings when the screen was operating. No transient phase was present in these records because the screen was running with material at the beginning of the test.

Figure 5.21 shows the acceleration time history in horizontal direction (CT001.XYO) for the case in which the screen is running with material. The data filtered by using the values are shown in Table 5.1. The maximum absolute acceleration and velocity is 0.040 g and 0.150 in/s. The maximum displacement is calculated as 0.018 in.

Figure 5.22 shows the Fourier spectrum for the horizontal direction, which shows the peak at the screen's horizontal frequency and influence of its vertical motion. The peaks shown in the Fourier spectrum includes peak frequency of 2.18 Hz. Fourier spectrum also shows peaks at the screen's horizontal and vertical frequency.

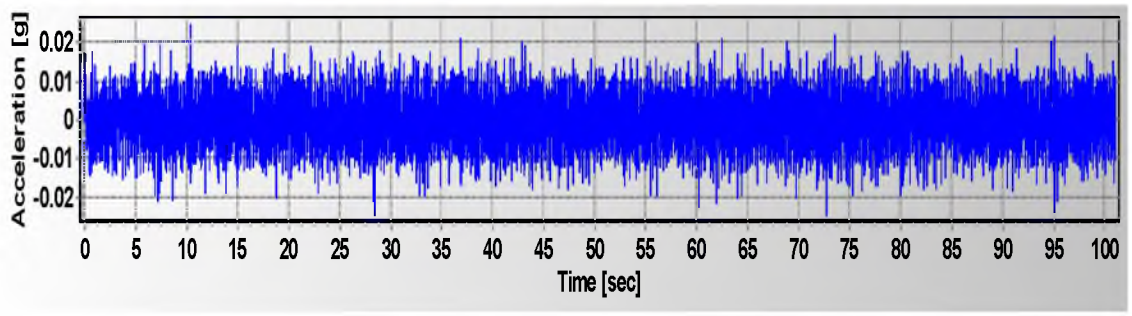

Figure 5.21 – Acceleration Time History of CT001.XYO

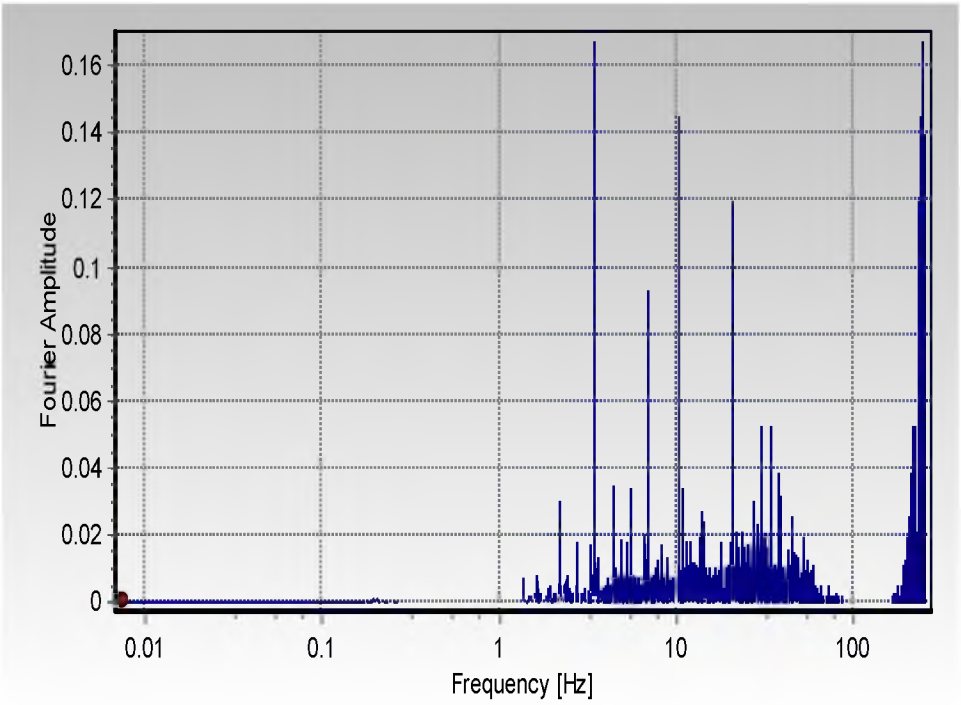

Figure 5.22- Fourier Spectrum of CT001.XYO

The response of the support system in orthogonal horizontal direction (y-direction) is shown in Figure 5.23.

The maximum absolute acceleration and velocity is 0.042 g and 0.19 in/s. The maximum horizontal displacement is calculated as 0.017 in. The Fourier spectrum shows the peaks at 1.91Hz and 13.74 Hz other than the harmonic frequencies. Figure 5.24 shows the Fourier spectrum of CT001.XY1.

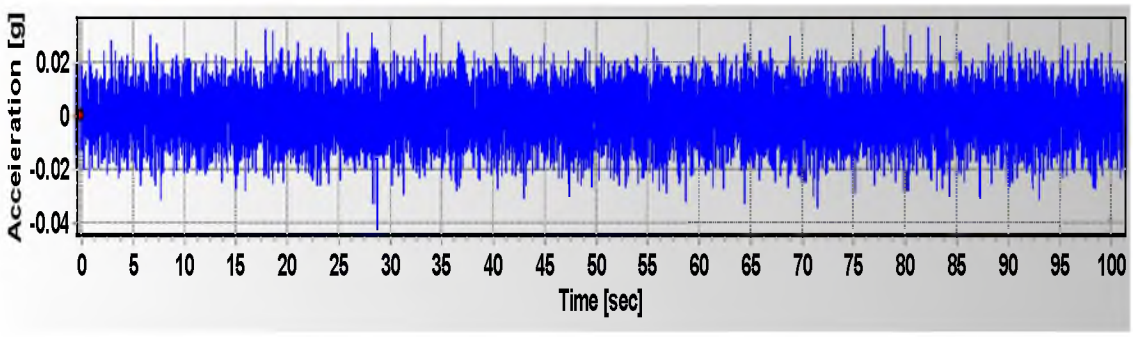

Figure 5.23 – Acceleration Time History of CT001.XY1

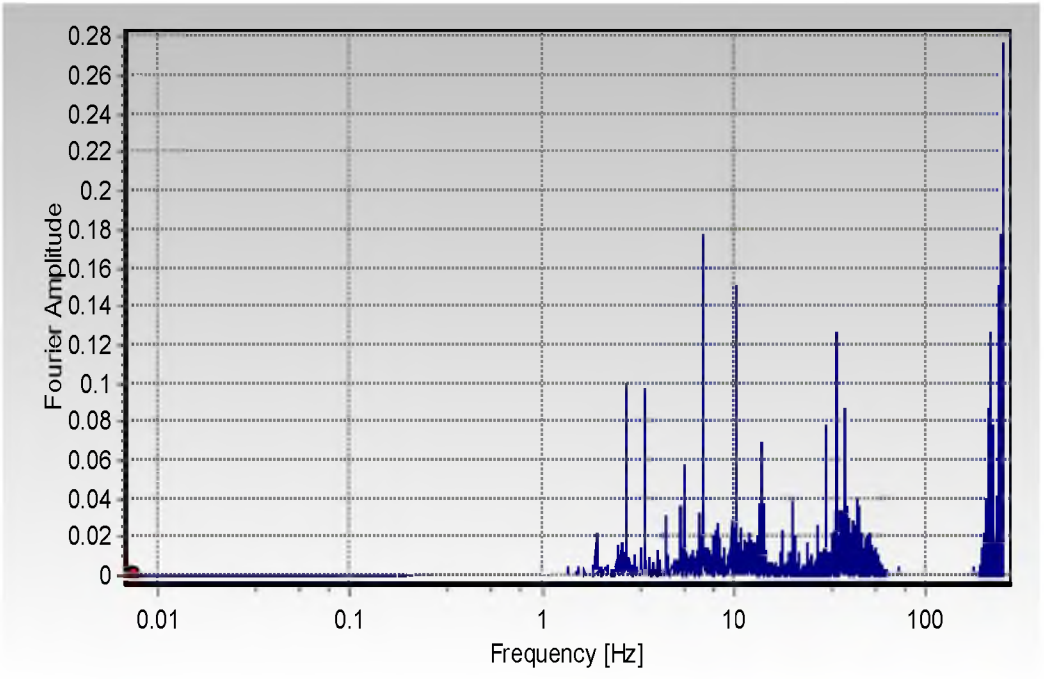

Figure 5.24 – Fourier Spectrum of CT001.XY1

The recording corresponding to the response in the vertical direction is named CT001.XY2. The acceleration time history of the vertical response is shown in Figure 5.25. The maximum absolute acceleration and velocity is 0.124 g and 0.330 in/s.

The maximum vertical displacement is calculated as 0.065 in. The Fourier spectrum is shown in Figure 5.26 and the peak is 13.74 Hz as well as at the operational frequencies of the screen.

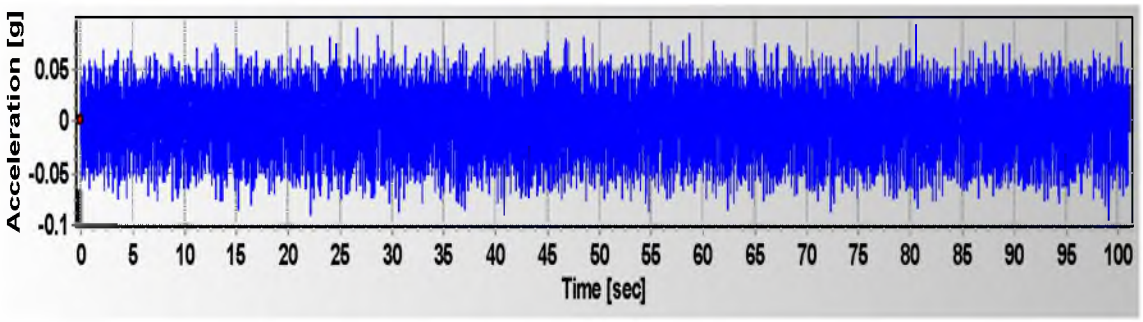

Figure 5.25 – Acceleration Time History of CT001.XY2

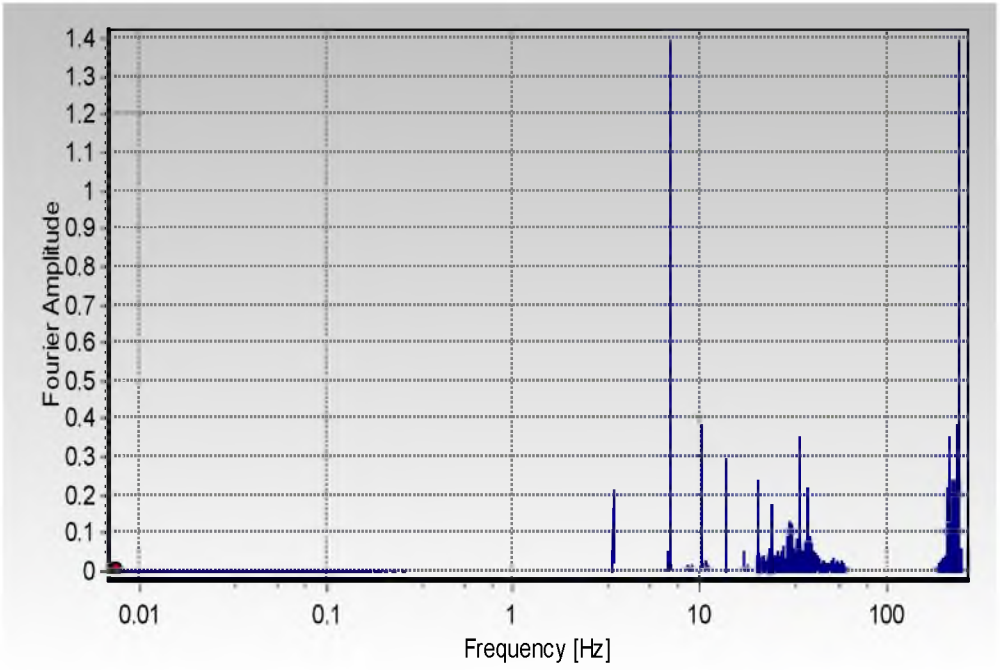

Figure 5.26 – Fourier Spectrum of CT001.XY2

6. DISCUSSION OF RESULTS

In this chapter, the results obtained from both numerical analyses and field experiments are compared. Several vibration guides are used to validate the data from numerical analyses and field experiments.

6.1. Comparison of Numerical and Experimental Results

6.1.1. Horizontal X-Direction

Table 6.1 represents the summary of results obtained from field experiments for the response in x- direction, including vibration amplitude (maximum absolute acceleration, velocity, and displacement, as well as peak frequency of the system. The vibration amplitude provides information about the status of the structure under dynamic loading.

The dynamic response in x- direction obtained from the modal analysis showed that the natural frequency of the system in x-direction is 1.92 Hz for empty and full case. From field experiments, Table 6.1 shows a peak frequency at 2.16 Hz and 2.18 Hz for empty and full case, respectively. This is a difference of 12.5% with respect to the numerical results.

Table 6.1 – Field Experiment Results for Three Cases in X-Direction

X-Direction	Maximum Absolute Acceleration	Maximum Absolute Velocity	Peak Frequency	Peak Period	Maximum Displacement
Ambient Case	0.005g	0.033 in/s	2.14 Hz	0.467 s	0.012 in
Empty Case	0.037g	0.150 in/s	2.16 Hz	0.463 s	0.015 in
With Material	0.040g	0.160 in/s	2.18 Hz	0.459 s	0.018 in

Another conclusion driven from the data shown in Table 6.1 is that the system's frequency in x-direction is not affected by the additional mass to the system. The difference between the peak frequency of empty and full cases is about 0.9%.

Figure 6.1 and 6.2 shows the displacement and acceleration history obtained from numerical analyses at the node where the readings are recorded. Figure 6.1 shows the displacement time history for the screen running with material. The maximum displacement is 0.020 in.

As shown in Table 6.1, the maximum displacement obtained from the field experiments is 0.018 in. Thus, the difference between the maximum displacement obtained from numerical analyses and field experiments is 0.002 in. That corresponds to a 10% difference between numerical and field results.

Also, Figure 6.2 shows the absolute acceleration response for the steady-state is 0.047 g. The acceleration response obtained from SAP2000 model is 15% more than the one from the experiments.

These comparisons show that the numerical models can predict the dynamic response of the screen's supporting frame with an error slightly of less than 10% for most parameters and conditions.

6.1.2. Horizontal Y-Direction

The dynamic response of the system from field experiments in y-direction is shown in Table 6.2. It includes the most common parameters used to identify the dynamic response, such as acceleration, velocity, displacement, peak frequency, and period.

The peak frequency obtained from field experiments is 2.16 Hz, whereas the peak frequency in y-direction for the screen with material is 13% less than the one for the empty case.

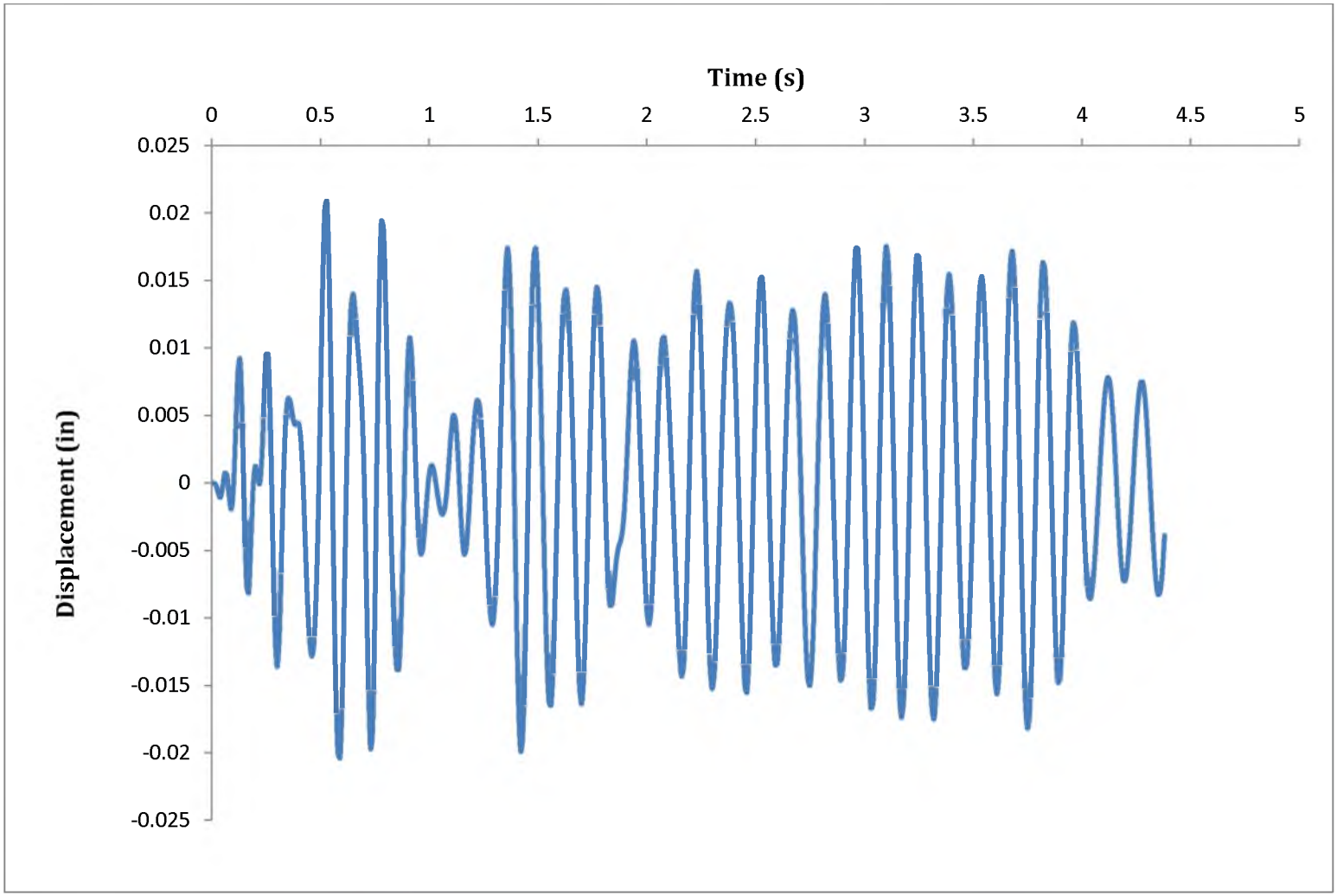

Figure 6.1 – Displacement Time History in X-Direction

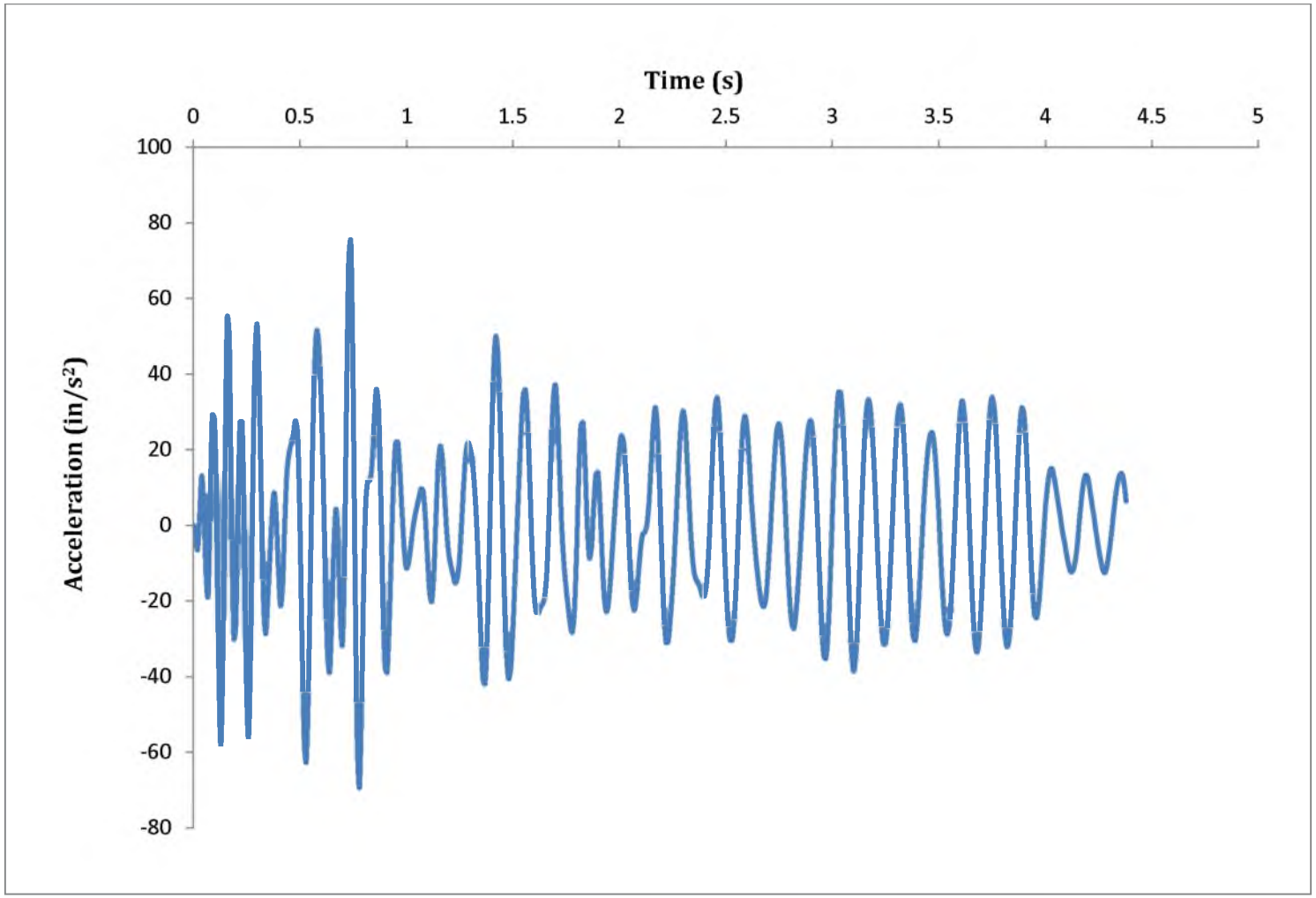

Figure 6.2 – Acceleration Time History in X-Direction

Table 6.2 – Field Experiment Results for Three Cases in Y-Direction

Y-Direction	Maximum Absolute Acceleration	Maximum Absolute Velocity	Peak Frequency	Peak Period	Maximum Displacement
Ambient Case	0.005g	0.045 in/s	2.04 Hz	0.490 s	0.012 in
Empty Case	0.038g	0.130 in/s	2.16 Hz	0.463s	0.016 in
With Material	0.042g	0.190 in/s	1.91 Hz	0.523 s	0.017 in

The natural frequency in y-direction is calculated as 2.16 Hz and 1.91 Hz for empty and full case, respectively.

The numerical analyses showed a natural frequency of 2.07 Hz in y-direction. Therefore, the frequencies obtained from numerical analyses differ approximately 5% from the ones obtained from experiments.

Figure 6.3 is the displacement time history in y-direction and the maximum displacement obtained from numerical analyses is 0.020 in. As shown in Table 6.2, the maximum displacement from field recording is 15% less than the numerical analysis response.

Furthermore, Figure 6.4 represents the acceleration time history in y-direction for the full case. After the transient response, the average acceleration is $0.039g$.

However, the maximum absolute acceleration from field experiments is 0.042g for the full case. That is, the difference is 7% between the numerical and field results, which indicates the numerical model is a good representation of the dynamic response of the steel frame.

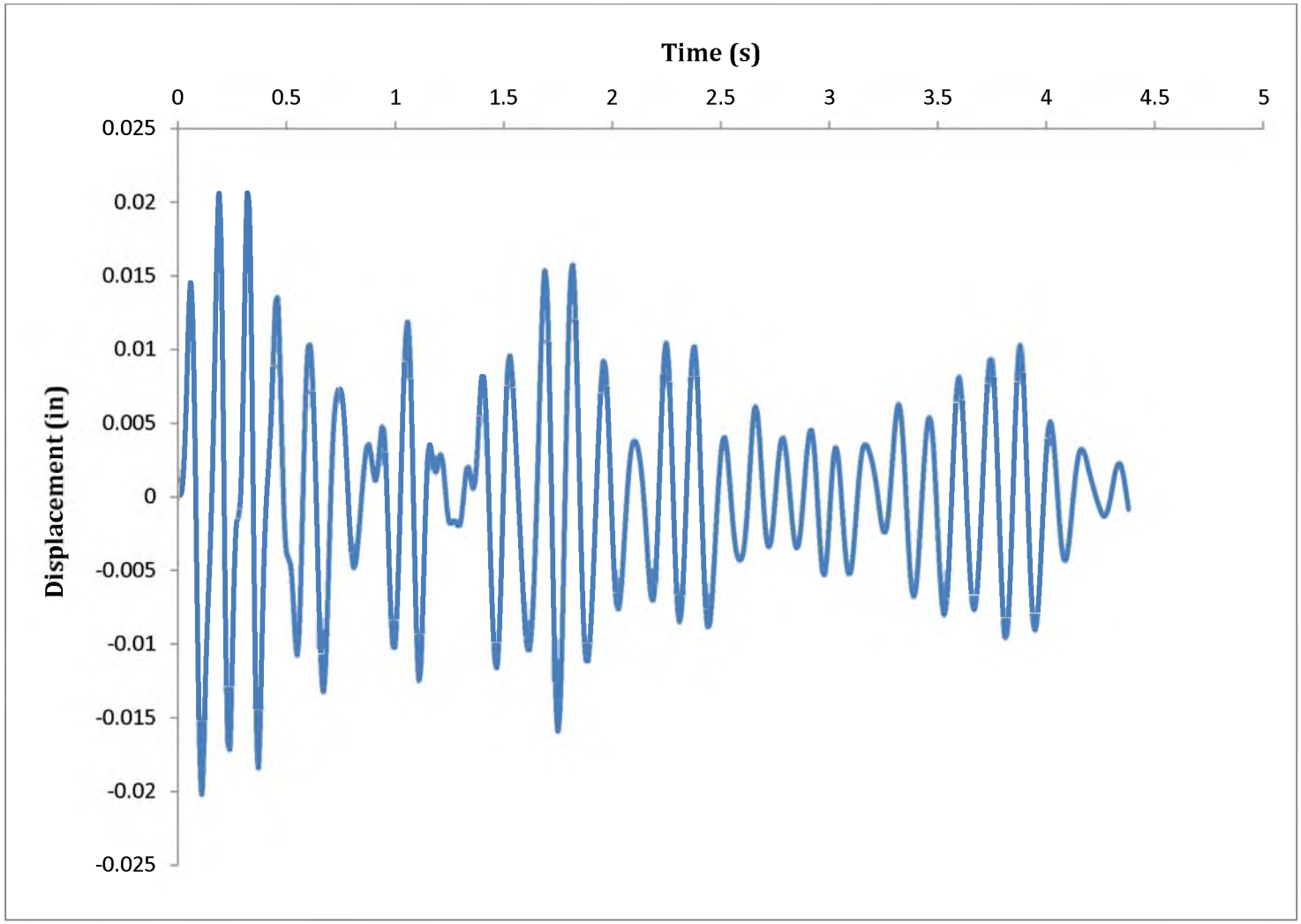

Figure 6.3 – Displacement Time History in Y-Direction

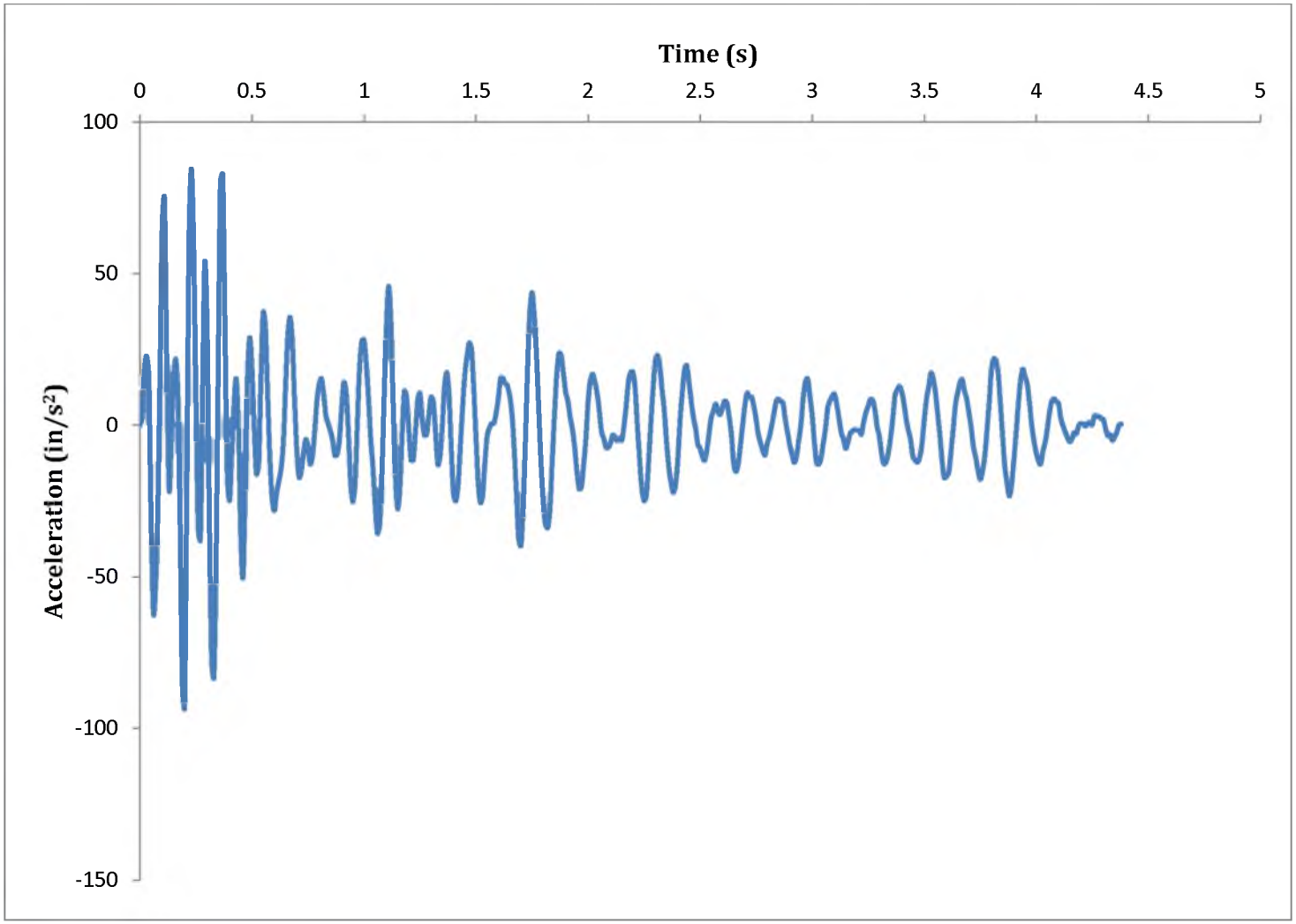

Figure 6.4 – Acceleration Time History in Y-Direction

6.1.3 Vertical Z-Direction

Table 6.3 summarizes the results obtained from field experiments in vertical direction; whereas Table 6.4 shows the natural vertical frequencies and corresponding periods calculated in numerical analysis for empty and full screen.

As in two horizontal directions, the peak vertical frequencies from experiments are almost the same, they only differ 0.4 % from each other. That is, the additional mass doesn't have a significant effect on vertical and horizontal frequencies.

For the empty case, the difference in the numerical and experimental frequencies is about 10%, a difference that drops to 2.8 % for the full case. As mentioned before, for the evaluation of vertical accelerations only the bay where the screen is attached to the building is modeled. The 6,400 lb-increase in mass is 40% increase in the screen's total mass which is not a small change when compared to the total mass of the vertical model of the support structure. That causes a 7.2% difference between empty and full case, which is large when compared to the horizontal results.

Table 6.3 – Field Experiment Results for Three Cases in Z-Direction

Z-Direction	Maximum Absolute Acceleration	Maximum Absolute Velocity	Peak Frequency	Peak Period	Maximum Displacement
Ambient Case	0.005g	0.028 in/s	9.38 Hz	0.107 s	0.002 in
Empty Case	0.133g	0.350 in/s	13.80 Hz	0.072 s	0.060 in
With Material	0.124g	0.330 in/s	13.74 Hz	0.073 s	0.065 in

Table 6.4 – Summary of Numerical Analysis for Z-Direction

	Vertical Frequency, $f_{n,v}$	Period, T_v
Empty Case	15.40 Hz	0.064 s
Full Case	14.14 Hz	0.071 s

Figure 6.5 is the displacement time history for vertical direction when the screen is running with material. The maximum displacement is 0.061 in. from the SAP2000 model. Table 6.3 shows a maximum displacement of 0.065 in., which corresponds to a 6% difference between numerical and experimental results. Figure 6.6 represents the acceleration time history for full case. The absolute steady-state acceleration response is $0.134g$, and the maximum absolute acceleration obtained from field experiments is $0.124g$. That corresponds to a 7.5% difference between numerical and field results. It indicates that the vertical model successfully simulates the support structure dynamic response.

6.2. Vibration Tolerance

After calculating and measuring the vibration amplitude of the system, it is important to check whether the vibrations are within tolerable limits. Although there are no widely accepted vibration limits, several guides provide recommendations for designers, such as the American Petroleum Institute (API), National Electrical Machinery Association (NEMA), International Standards Organization (ISO) and the classes of machinery causing the vibratory action and ISO Guideline for Machinery Vibration Severity are given in Figure 6.7 and Figure 6.8, respectively. The Hydraulic Institute. . It shows the status of the system for a given velocity. Rotex screen is Class IV machinery due to its flexible connections to its supporting structure.

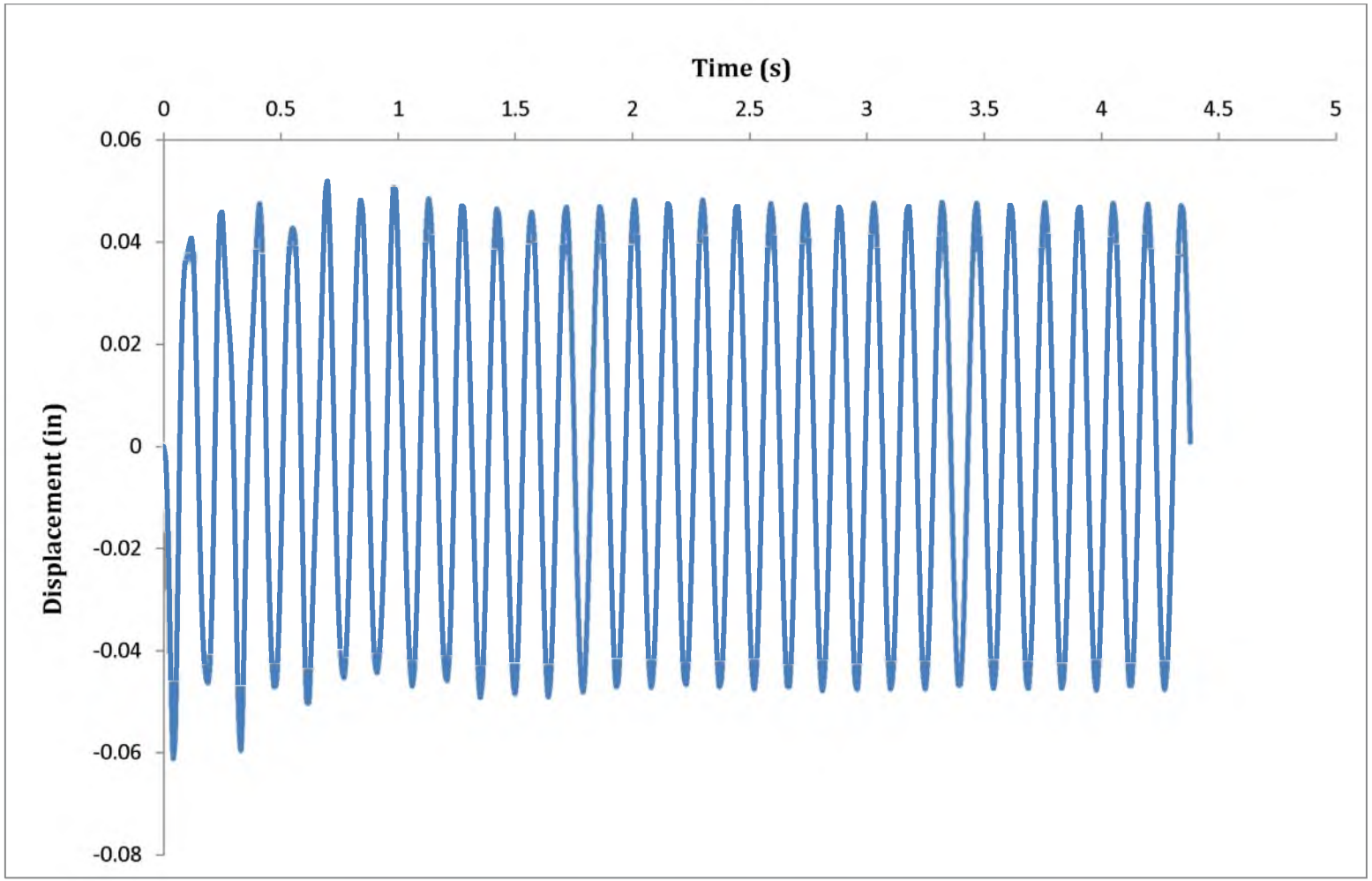

Figure 6.5– Displacement Time History in Z-Direction

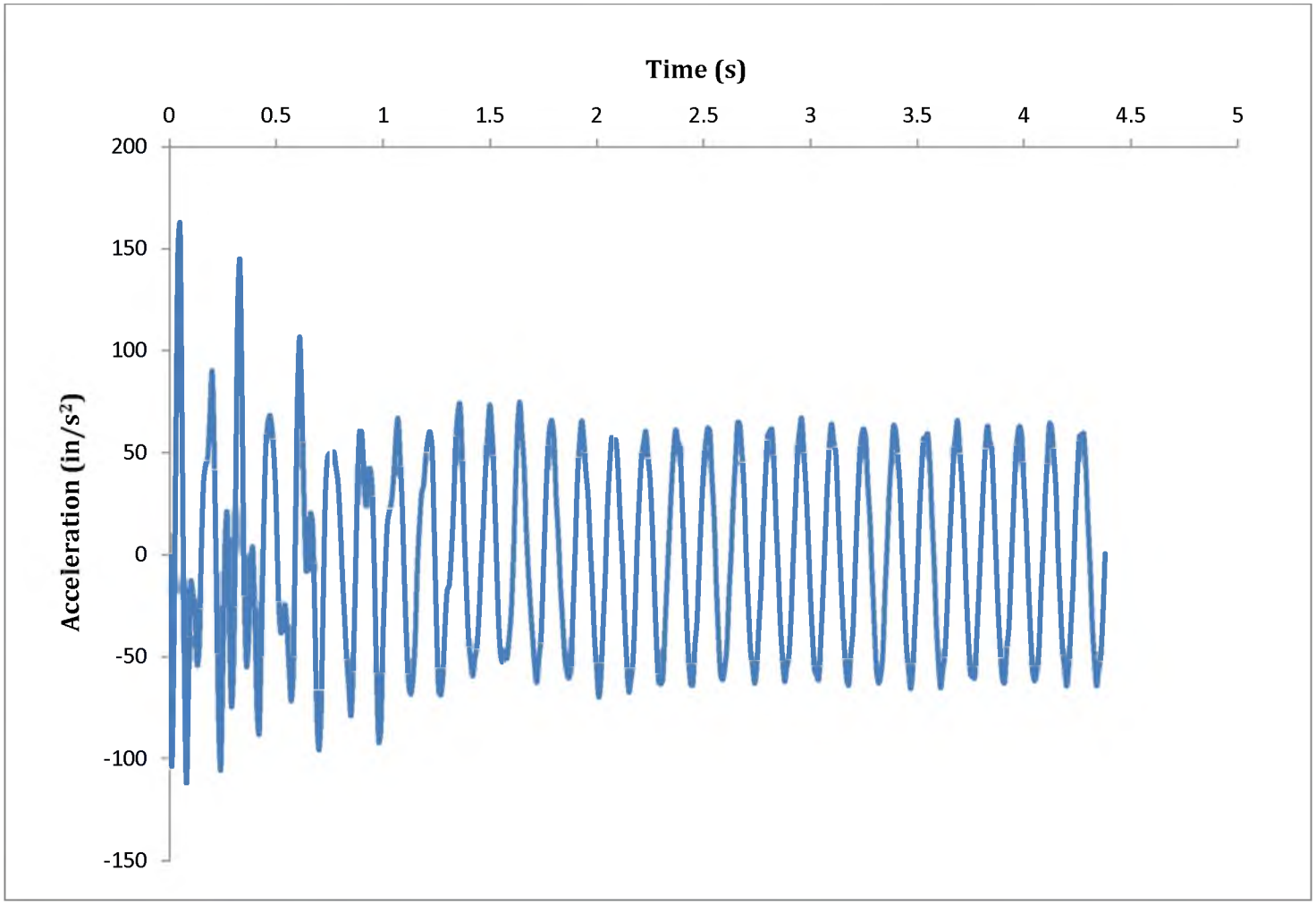

Figure 6.6 – Acceleration Time History in Z-Direction

Class I	Individual parts of engines and machines integrally connected with a complete machine in its normal operating condition (production electrical motors of up to 15 kW are typical examples of machines in this category).
Class II	Medium sized machines (typically electrical motors with 15-75 kW output) without special foundations, rigidly mounted engines or machines (up to300 KW) on special foundations.
Class III	Large prime movers and other large machines with rotating masses mounted on rigid and heavy foundations, which are relatively stiff in the direction of vibration.
Class IV	Large prime movers and other large machines with rotating masses mounted on foundations, which are relatively soft in the direction of vibration measurement (for example- turbo generator sets, especially those with lightweight substructures.

Figure 6.7 – Classes of The Machines Corresponding to ISO 2372

ISO2372- ISO GUIDELINE FOR MACHINERY VIBRATION SEVERITY					
RANGES OF VIBRATION SEVERITY		EXAMPLES OF QUALITY JUDGMENT FOR SEPARATE CLASSES OF MACHINES			
Velocity -in/s	Velocity-mm/s	Class I	Class II	Class III	Class IV
-Peak	-RMS				
0.015	0.28				
0.025	0.45				
0.039	0.71				
0.062	1.12				
0.099	1.8				
0.154	2.8				
0.248	4.5				
0.392	7.1				
0.617	11.2				
0.993	18				
1.54	28				
2.48	45				
3.94	71				

A- Good
B-Acceptable
C-Not Acceptable

Figure 6.8 – ISO Guideline For Machinery Vibration Severity

As shown in Table 6.1, the maximum absolute velocities in x-direction for empty and full case are 0.140 in/s and 0.150 in/s, respectively. Comparing the maximum velocities with the values given in Figure 6.8 indicates the severity of the vibration level the system is experiencing. Therefore, the system falls into the Category B corresponding to an "acceptable" level of vibration for the velocities in x-direction. For y-direction, the maximum absolute velocities are 0.130 in/s and 0.190 in/s for the empty and full case, respectively. According to Figure 6.8, the system for each case is in Category B, which corresponds to an "acceptable" level of vibration. For z-direction, the maximum absolute velocity is measured as 0.350 in/s for empty case; whereas, it is 0.330 in/s for the screen running with material. Even for these higher velocity values, the system still stays in Category B, which requires no action to take. In addition, using Vibration Severity Chart by Baxter and Bernhard (1967), Reiher-Meister Chart by Richart, et al., (1970), and the vibration limits obtained by Sandwell (2012), Table 6.5 and Table 6.6 is constructed. Table 6.5 and Table 6.6 represent the acceleration and velocity structural vibration limits. In this study is indicated that using both velocity and acceleration as vibration severity measure is applicable to all types of general rotating equipment. Therefore, the tables can be used as a reference for vibration tolerances because the screen falls into the rotating machinery category.

According to Table 6.5, the structure is in excellent condition considering the acceleration in x and y direction; whereas, it falls into good condition category for the acceleration in z-direction. No action is required considering these results. According to the velocity values given in Table 6.6, for both horizontal directions, the structure is in good condition. However, in vertical direction, the support structure is in a tolerable condition. No action is required, unless it is noisy. The acceleration and velocity limits defer slightly. However, none of the conditions that the structure is experiencing require changes.

Table 6.5 – Acceleration Limits for Structural Vibration

Acceleration Limits		
a< 0.10g	Excellent Levels	No action required.
0.10g <a< 0.35g	Good Levels	No action required unless noisy.
0.35g <a< 0.50g	Fair Levels	No action required unless noisy.
0.50g <a< 0.75g	Rough Levels	Possible action required. Check bearing noise and temperature.
0.75g <a< 1.00g	Very Rough Levels	Further Analysis required.
1.00g <a< 1.50g	Danger Levels	Failure is near.
a> 2.50g	Failure Levels	Shut it down immediately.

Table 6.6 – Velocity Limits for Structural Vibration

Velocity Limits		
v< 0.10 in/s	Excellent Levels	No action required.
0.10 <v< 0.20 in/s	Good Levels	No action required unless noisy.
0.20 <v< 0.30 in/s	Fair Levels	No action required unless noisy.
0.30 <v< 0.40 in/s	Tolerable Levels	No action required unless noisy. Check bearing noise and temperature.
0.40 <v< 0.60 in/s	Rough Levels	Take action now.
v> 0.60 in/s	Danger Levels	Shutdown and fix.

7. CONCLUSION

7.1. General

The identification and suppression of excessive vibration in industrial structures is important to improve productivity by preventing downtimes or components failure. This thesis increases the knowledge of the dynamic behavior of steel frame structures subjected to the harmonic loading caused by rotating machinery (i.e., screens). Computer-aided analyses and field experiments are performed to better understand the vibration transferred from the screen to its supporting structure. The results are compared and discussed to obtain an accurate modeling process.

The objectives of this study are to determine the parameters controlling the structural response, and to provide practical methods to eliminate excessive vibrations on the steel frames at the design stage. It is concluded that:

- The weight of the material in the screen has a negligible effect on the system's frequency; even in the vertical direction due to the pendulum effect (the screen's elliptical movement causes the material float).
- The vertical vibrations can be evaluated in isolation considering only the bay where the screen is located. The simply supported beams tend to isolate the vertical vibration from the rest of the structure.
- The vertical vibrations tend to be a local phenomenon, whereas horizontal vibrations are related to the overall building's response.
- The horizontal dynamic displacements caused by the screen should not be significant because the screen's mass is very small compared to the building's mass,

and the forcing frequency (f_h= 3.43 Hz or $T_h = 0.29\ s$) is relatively higher than the horizontal natural frequency of the steel frame structures with no rigid diaphragms.

7.2. Recommendations

There are some recommended check points for the vibration design of the systems that support vibrating machinery. These check points depend on the results obtained from the modal response analysis and the acceleration time history analysis.

Modal response analysis provides the natural vertical and horizontal frequency of the system from numerical models. From the ratio of the natural frequency to the forcing frequency, the amplification in the dynamic response can be calculated. In addition, the time history analysis provides the displacement, acceleration and velocity response of the system which provides evaluation of the vibration level that the system is exposed to.

For conventional steel grating slabs in steel frames, the natural frequency is in the range of the vertical forcing frequency of the screen. Thus, these systems have to be designed to have a vertical natural frequency that is different from the screen's vertical frequency.

The recommended frequency ratio $f_v/f_{n,v}$ is given in Table 7.1. In addition, zone 1 in Figure 7.1 represents the ratio of vertical forcing frequency-to-natural vertical frequency for a reliable design.

Steel frame buildings are likely to have a smaller natural horizontal frequency than the screen's horizontal forcing frequency, 3.43 Hz (T= 0.29 s). Therefore, Zone 2 in Figure 7.1 represents the recommended horizontal frequency ratio for the steel frame buildings. In addition, Table 7.1 represents the recommended frequency ratio for the horizontal direction. Note that the main parameter that can be controlled in design is the rigidity of the system.

Table 7.1 – Recommended Frequency Ratios

Vertical:	$f_v / f_{n,v} \geq 2 \quad or \quad f_v / f_{n,v} \leq 0.5$
Horizontal:	$f_h / f_{n,h} \geq 2 \quad or \quad f_h / f_{n,h} \leq 0.5$

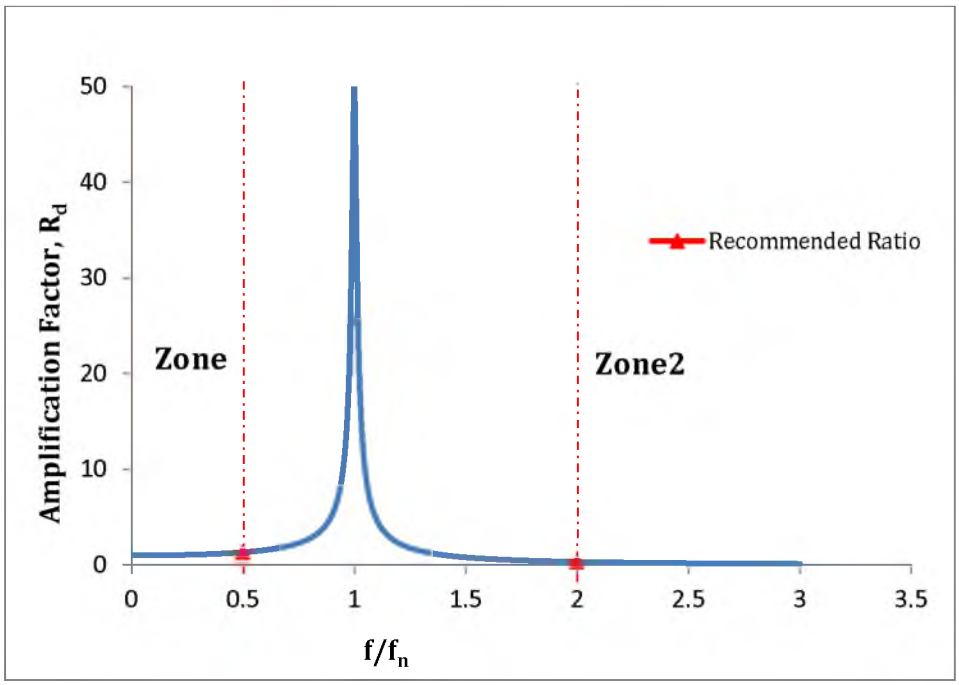

Figure 7.1- Recommended Sides for $f_v/f_{n,v}$ and $f_h/f_{n,h}$

Shifting the system to the safe zone can be achieved by adjusting the frequency ratio for vertical and horizontal case. For vertical case, the recommended action is either to increase the stiffness of the system or to decrease the mass only if the ratio is on the left side of the peak shown in Figure 7.1. In this case, increasing the stiffness of the system is recommended. On the other hand, if the frequency ratio is on the right side of the peak as in the horizontal case, either the mass of the system should be increased or the stiffness should be decreased.

For this case, adding mass to the system can be more convenient unless shifting the frequency ratio to the left side of the peak by increasing the stiffness is possible.The time history results are indicated as a second check point for a reliable design, the responses obtained from time history analysis such as acceleration and velocity, are evaluated by using the vibration tolerance charts given in section 6.2.

7.3. Future Considerations

As a practical design solution, only structural modifications were considered in this study. The structure investigated was under excessive vertical vibration caused by screen and the structure was already completed. In addition, the manufacturer of the screen did not recommend using any other passive vibration control methods such as absorbers, isolators or dampeners. Therefore, utilizing structural modification was the most convenient solution. However, for future studies, it would be beneficial to research the effects of the vibration isolators on the screen's supporting frame.

Secondly, the dynamic response of one screen is evaluated in this study, but it is likely to have more than one screen operating on the same floor. Under that circumstance, it would be beneficial to research the effects of multiple screens on the dynamic response when they run at the same time.

APPENDIX A

TRUSS SECTIONS

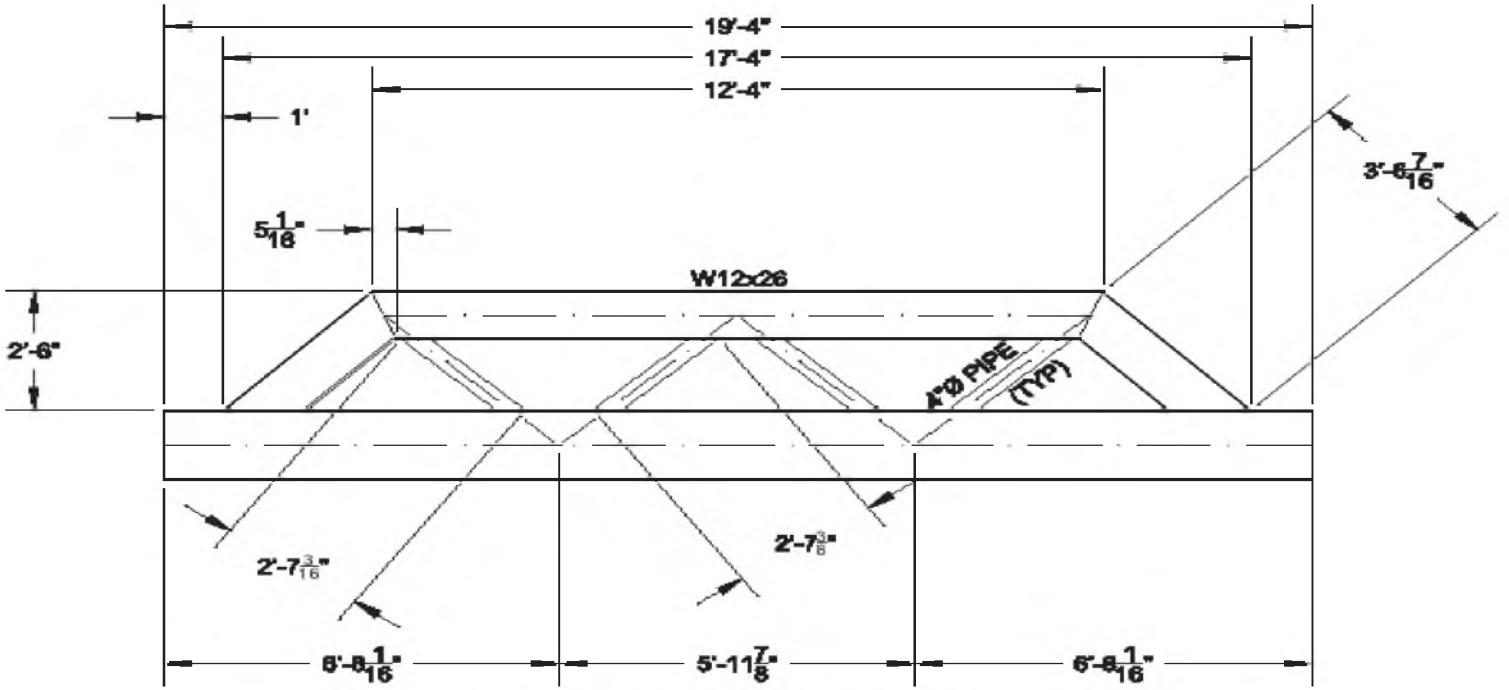

TRUSS OVER W18 (RUNNING E-W)

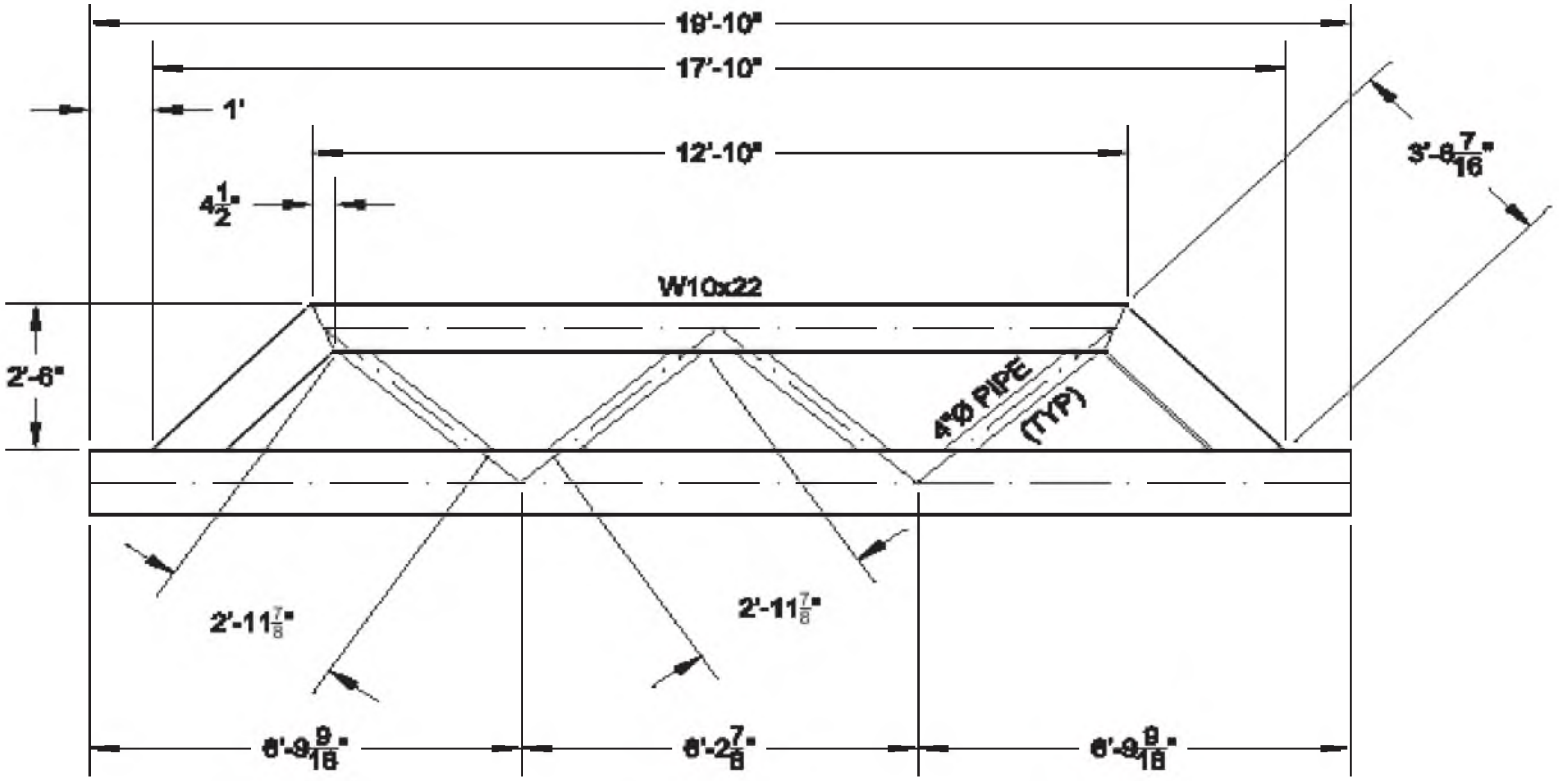

TRUSS OVER W14 (RUNNING N-S)

The truss section shown above represents the members that are welded on top of the beams to which the screen is attached.

APPENDIX B

BASELINE CORRECTION AND FILTERING

B.1. Frequency Filtering

Filtering is used to decrease the frequency range from a given signal to prevent unwanted frequency components from the data. In the software used in this study, SeismoSignal (2012), the filter configuration used is defined as follows:

i. Lowpass filtering removes the frequencies that are higher than a user-defined frequency (Freq1).

ii. Highpass filtering removes the frequencies that are less than the cut-off frequency (Freq1).

iii. Bandpass filtering considers signals in a given frequency range (Freq1 to Freq2) bandwidth. Bandpass filtering configuration is used in this study.

iv. Bandstop filtering removes signals which are out of the given frequency range (Freq1 to Freq2).

Infinite-impulse-response (IIR) filter types are used in SeismoSignal to create the four filtering configurations defined previously. These three filter types are Butterworth, Chebyshev and Bessel.

Butterworth filter type can be used for most of the applications due to its flat response in the passband. However, it causes smaller roll-off steepness when compared to a Chebyshev filter of the same order. Using a higher order filter can eliminate the roll-off steepness and the adequate amount of high filtering can be determined by sensitively

adjusting the order of the polynomials from 1st up to the 8th order. Chebyshev filter refers to the passband configuration which leads to a faster frequency roll-off. The value for the passband ripple can be determined by the user. Bessel filter is the slowest frequency roll-off amongst all three filter types an it requires the highest order to meet an attenuation specification.

In this study, Butterworth is used as a filter type due to its flat response in the passband, in addition, Bandpass is preferred for the filter configuration with 4th order polynomial coefficients.

B.2. Baseline Correction

Instrumental measurements usually have unstable baselines, which can create a smooth baseline and a series of peaks consisting of negative or positive peaks. Baseline correction is often used to eliminate these problems and create a stable baseline. Baseline Correction is used for

(i) "Determining, through regression analysis (least-squares-fit method), the polynomial curve that best fits the time-acceleration pairs of values and then

(ii) Subtracting from the actual acceleration values their corresponding counterparts as obtained with the regression-derived equation. In this manner, spurious baseline trends, usually well noticeable in the displacement time-history obtained from double time-integration of uncorrected acceleration records, are removed from the input motion" (SeismoSignal, 2012).

The polynomial degree can be determined by the user and polynomials of up to the 3rd degree can be used for baseline correction.

REFERENCES

Allis-Chalmers. Vibrating machinery: Calculating supporting structures. **1968.**

Ambrosini, R., Curadelli, R., & Danesi, R. Alternative to traditional systems of vibration control of rotating machinery. *Journal of Process Mechanical Engineering*. **2005**, *219*, 27-42.

American Institute of Steel Construction. *Steel Construction Manual*, 14th ed.; Chicago, 2011.

American Concrete Institute. *ACI Manual of Concrete Practice Part 4*; Farmington Hills: Michigan, 2012.

Arpaci, A. Annular Plate Dampers Attached to Continuous Systems. *J. Sound Vibr.*, **1996**, *191*, 781-793.

Assunção, T. M. R. C. Considerações sobre efeitos dinâmicos e carregamentos induzidos por fontes de excitação em estruturas. Master's thesis, Federal University of Minas Gerais, Minas Gerais, MG, Brazil, 2009.

Bachmann, H., & Ammann, W. Vibration in structures induced by man and machines. City University of Hong Kong [Online], **1987**. http://personal.cityu.edu.hk/~bsapplec/transmis3.htm (accessed August, 2012).

Chopra, A. *Dynamics of structures: Theory and applications to earthquake engineering*. Editorial Prentice Hall: New York, 2006.

Eilers, P., & Boelens, H. Baseline correction with asymmetric least squares smoothing. University of Amsterdam, Netherlands. [Online] **2005**. http://www.science.uva.nl/~hboelens/publications/draftpub/Eilers_2005.pdf (accessed September, 2012).

Harris, C., Piersol, A. *Harris' shock and vibration handbook*. McGraw-Hill: New York. 2002.

Humar, J. *Dynamics of structures*. Swets & Zeitlinger B.V.: Lisse. 2002.

Girdhar, P. *Practical machinery vibration analysis and predictive maintenance*. Elsevier: Massachusetts. 2004.

LDS Datron. Basics of structural vibration testing and analysis: Application note an011. [Online] **2003**. http://www.calpoly.edu/~cbirdson/Publications/AN011 Basics of Structural Testing Analysis.pdf (accessed July, 2012).

Modarreszadeh, M. Dynamic analysis of structures with interval uncertainty. Doctoral dissertation, Case Western Reserve University. 2005.

Prakash, S., & Puri, V. Foundations for vibrating machines. *Journal of Structural Engineering India*. **2006**, *Special Issue*.

Rakesh, K., & Chopra, A. Period formulas for moment-resisting frame buildings. *Journal of Structural Engineering*, **1997**, *123.11*.

Remington, P., Allik, H., & Martin, N. Static design and dynamic analysis of light weight machinery support structures. *ASME*. **1995**, *3(B)*.

Rimola, B., Silva, J., Sieira, A., & Lima, L. Vibration analysis of an oil production platform. *Associación Argentina de Mecánica Computacional*. [Online] **2010,** *29*, 7529-7540. http://www.cimec.org.ar/ojs/index.php/mc/article/viewFile/3541/3454 (accessed July, 2012).

Robichaud, J. Reference standards for vibration monitoring and analysis. http://www.bretech.com/reference/Reference Standards for Vibration Monitoring and Analysis.pdf (accessed September, 2012).

Ronlov, S. Vibration problems in ore processing plants. *Transactions, Society of Mining Engineering*. **1962,** *223*, 278-284.

ROTEX. *Mineral seperators*. http://www.rotex.com/products/screeners-separators/rotex-minerals-separator (accessed May, 2012).

Sandwell, G. Learn about vibration: Basic understanding of machinery vibration.*VIBES Corp* **2012**. http://www.vibescorp.ca/pdf/basic_understanding_of_machinery_vibration.pdf (accessed September, 2012)

SAP2000, version 15.1; Structural Analysis Software: Berkeley, CA, 2012 (accessed May, 2012).

SeismoSignal, version 5; Earthquake Engineering Software: Italy, 2012 (accessed July, 2012).